Extracting implied volatilities from bank bonds

Extracting implied volatilities from bank bonds

Michele Leonardo Bianchi[a,1], Gian Luca Tassinari[b,1]

[a] *Financial Stability Directorate, Bank of Italy,*
micheleleonardo.bianchi@bancaditalia.it
[b] *Department of Management, University of Bologna,*
gianluca.tassinari2@unibo.it

This version: June 13, 2023

Abstract. In this work we explore the information content of senior, subordinated and additional tier 1 (or contingent convertible) bonds issued by euro area banks. We analyze both the asset volatility implied in senior and subordinated bonds and credit default swap market spreads, and the common equity tier 1 (CET1) ratio volatility extracted from additional tier 1 bonds secondary market spreads in the period from December 31, 2012 to March 31, 2021. Furthermore, we jointly consider the following important bank variables: asset, equity and CET1 ratio volatilities. In doing so, we can obtain the market view on credit spreads, banks balance sheet and capital ratio dynamics on a daily basis even if bank data are released quarterly. The approach can be used to monitor the risk of each bank, as perceived by the market, and to investigate banking fragility at a stand-alone or at a country level. Finally, we compare our estimated equity implied volatilities with the volatilities implied in equity option quotes and we show that this indicator depends on the model and the financial instruments considered in the calibration.

Keywords: subordinated bonds, AT1 bonds, CoCo bonds, credit default swaps, capital requirements, CET1 ratio, implied CET1 volatility, firm value models.

JEL: C02, G12, G21.

[1] The authors are grateful to Pierluigi Bologna, Emilia Bonaccorsi di Patti, Antonio Di Cesare, Arianna Miglietta, and two anonymous referees for their helpful suggestions. The views expressed are those of the authors and do not necessarily reflect those of the Bank of Italy.

1 Introduction

The secondary bond market and the related credit derivative contracts are a rich source of information for analyzing the risk of the issuers (Conciarelli [2014], and Bianchi and Rocco [2016]). Even if there are dozens of different types of bonds, the bonds issued by banks can be divided into three main categories: senior, subordinated (or Tier 2) and additional tier 1 (AT1) or contingent convertible (CoCo) bonds moving from the less risky senior bonds to the almost equity-like AT1 bonds. Recently, the non-preferred senior class was introduced to allow European banks to meet the minimum requirements for own funds and eligible liabilities (MREL). Moreover, these bonds help European global systemically important banks (G-SIBs) to meet the total-loss absorbing capacity (TLAC) requirement. Sometimes they are referred to as Tier 3 even if they are not regulatory capital instruments (see Liberadzki and Liberadzki [2019]). Since the non-preferred bond market is in its early stage, we do not analyze it in this work.

In this paper we propose a bond pricing framework that takes into account credit spreads of senior, subordinated and CoCo debts, bank balance sheet data and prudential information on capital ratios. More precisely, we empirically assess and extend the works of Hilscher and Raviv [2014] and De Spiegeleer et al. [2017] under different perspectives: (1) we define a framework which, consistently with the structure of a bank balance sheet, is able to connect and extract asset, equity and CET1 ratio volatilities; (2) we explore the dynamics of the CET1 ratio by following an approach similar to that of Choe et al. [2019]; (3) we conduct an extensive empirical analysis on the main European banks and estimate various indicators useful for risk analysis.

Most of the literature related to our paper is mainly theoretical and lacks an empirical assessment on real balance sheet and market data (e.g. Hilscher and Raviv [2014] and Choe et al. [2019]). In other cases, the focus is narrow as they only consider the estimation of a single volatility indicator (e.g. Lovreta and Silaghi [2020] studied the asset volatility and De Spiegeleer et al. [2017] defined the CET1 ratio volatility). Conversely, we adopt a broader perspective by linking asset, equity and CET1 ratio volatilities under a unified framework and show their dynamics over an extensive period of time. The empirical analysis is based on real balance sheet and market data from December 31, 2012 to March 31, 2021 for the main European banks. It reveals that our model works properly since its calibration error, on average, is small (at least for the trading days considered in this study). We also show that the estimates of the implied equity volatility depend on the model and the financial instruments considered in the calibration.

While the history of senior and subordinated instruments is not recent, the first CoCo note was issued by Lloyds in late 2009 and the current definition of AT1 bonds came into force only in 2014 with the Capital Requirements Directive (CRD) IV package. De Spiegeleer et al. [2014], Liberadzki and Liberadzki [2016], Liberadzki and Liberadzki [2019] and Oster [2019] have provided a detailed and complete discussion on CoCos. Boermans and van Wijnbergen [2018] studied European CoCos holders from a financial stability perspective and concluded that cross-holdings of CoCos by euro area banks are negligible. Bologna et al. [2020] analyzed the dynamics of the European CoCos market during two distress episodes in 2016, triggered by a European systemic bank, with the aim to disentangle a fundamental contagion channels from a potential CoCo-specific contagion channel.

As observed by Kjell and Nicolas [2014], Fuentes and Casado [2017] and Resti [2016] the Basel III capital accord and the regulation on recovery and resolutions are increasing the need for credit institutions to have a sufficient capital buffer to absorb potential losses. CoCo bonds can potentially contain valuable information on the soundness of the issuer making these instruments interesting from a monitoring perspective. After having analyzed the liquidity on the CoCo market, Grinderslev and Kristiansen [2017] explored the price dynamics of these bonds and studied their correlation with equity prices. Kazato and Yamada [2018] proposed a model to extract bail-in probabilities from CoCo spreads.

However, the pricing of these bonds is complex since they have many embedded options, such as conversion of the principal subject to the breach of a trigger, cancellation of the coupons and extension of the maturity. Complexity is amplified by the fact that triggering may be taken on a discretionary basis by the supervision or resolution authority (see Glasserman and Perotti [2018] for a discussion on this topic).

Various pricing models have been analyzed in De Spiegeleer et al. [2014], Oster [2019] and references therein. Buergi [2013] discussed the fundamentals of CoCo pricing and described possible problems that arise when attempting to price CoCos with an accounting (or capital ratio) trigger. Hilscher and Raviv [2014] defined a firm value model able to deal with the different types of banks liabilities. Specifically, assuming the existence of a constant continuously compounded risk free rate and a geometric Brownian motion to model assets dynamics, they derived the price of all banks liabilities and equity in closed-form by evaluating different replicating portfolios consisting of barrier options. Brigo et al. [2015] proposed a pricing methodology based on firm value models allowing to calibrate exactly the credit term structure of the issuer and derived the equity value in closed form with a barrier option type formula. Additionally, they introduced decorrelation between the capital conversion trigger and the credit quality of the issuer. De Spiegeleer et al. [2017], by looking at CoCo bonds as a kind of barrier product where coupons are cancelled and the trigger is activated when a CET1 barrier is breached, introduced the concept of implied CET1 volatility. De Spiegeleer et al. [2018] analyzed these products under a risk management perspective. Specifically, after providing an overview of the risk components of a CoCo bond, they derived different market implied pricing models and created more insights into the instruments sensitivities. Recently, Choe et al. [2019] proposed two approaches for pricing capital-ratio trigger CoCo bonds: while the former approach was based on the stock price and the capital-ratio dynamics, the latter approach was based on the equity and the total risk weighted assets (RWA) value processes.

As observed by Lovreta and Silaghi [2020], even if in structural credit risk models firm assets volatility is one of the key determinants of default probabilities, bonds and credit derivatives prices, surprisingly little is known about the behavior of this variable. Recently, various authors started studying this topic. By inverting the CreditGrades model, Byström [2016] backed out credit-implied stock prices and stock return volatilities from credit default swap spreads. Russo et al. [2019] provided a methodology, based on Merton model under stochastic interest rates, to infer market implied volatilities for defaultable bonds using equity implied volatilities and CDS spreads. Kelly et al. [2019] defined and constructed a credit-implied volatility surface from the firm-by-maturity panel of CDS spreads. Similarly, Lovreta and Silaghi [2020], by following the approach originally proposed by Forte [2011], analyzed the behavior of asset implied volatilities under a structural model of default and by backing-out asset implied volatility from observed CDS spreads.

Readers are referred to Augustin et al. [2016] for a review of the literature on CDS in the aftermath of the financial crisis (see also Forte and Lovreta [2023]).

As in most of the studies on this subject, our model does not allow for jumps in asset, equity or CET1 ratio. Even if the model can be theoretically extended to Lévy processes capable of modeling jumps and of generating leptocurtic and asymmetric distributions (see Hieber and Scherer [2012] and Kim [2019]), we want to keep our framework as simple as possible to get closed formulas for default and CoCo trigger probabilities, bonds and stocks prices.

Although from a theoretical and experimental perspective (i.e., in which parameters value is imposed and sensitivity analyses are performed), the use of an exponential Lévy process for the total asset value is possible, from a more practical point of view the limited observability of the total asset value, once in each quarter, makes the direct estimation of the asset dynamics infeasible and the implementation of a model based on non-Gaussian Lévy processes extremely challenging. In models with jumps it is usually not possible to obtain closed-form expressions for spreads, default and CoCo trigger probabilities and simulation procedures are needed to calibrate the parameters. Furthermore, simulation procedures of continuous-time processes require a discretization of the time dimension and this introduces additional bias. Lastly, given the data availability, the increase in the number of parameters due to the use of Lévy processes with jumps makes the estimates less robust.

In this paper, we consider a less complicated and more parsimonious framework based on the geometric Brownian motion, avoiding in this way to resort to simulation methods that make calibration rather difficult, time consuming, and less accurate. Under our framework, closed formulas for spreads, default and CoCo trigger probabilities allow to calibrate the model on real data by minimizing functions that explicitly depend on the unknown parameters to be estimated. We believe that the approach described in this paper represents a good compromise between tractability and realism.

The paper is structured as follows. In Section 2, we describe our pricing framework and show how to extract the asset volatility from bonds or CDS spreads. In Section 3, a review of the CET1 volatility approach is provided. In Section 4, the relations between asset, equity and CET1 volatility are studied under a theoretical perspective. In Section 5, we describe the financial instruments and data considered in the empirical study. Section 6 is devoted to the empirical analysis and provides more information on the calibration approach, together with a discussion on the results. In Section 7, we show how to monitor bank fragilities at individual or country level. Section 8 concludes. The derivation of the main formulas is provided in the Appendix.

2 Bond pricing models

We consider a bank with total asset value at time t, A_t, following a geometric Brownian motion with volatility parameter σ_A. To finance its assets, the bank has five types of claims: a single zero-coupon deposit, a senior, a subordinated, and a contingent convertible debt, and a residual equity claim. Following the approach of Hilscher and Raviv [2014], we assume that all liabilities mature at time T, unless there is a security specific event previous to time T. In Section 2.1, we describe how to compute the price of senior

bonds, subordinated bonds, and equity in a firm value model of a bank not having contingent convertible bonds. Then, in Section 2.2 we consider a bank having all five types of claims.

Before describing the models, we want to focus attention on the formula needed to compute the spread of a bond starting from its price. The spread at time t of a zero-coupon bond with price $B(t,T)$, face value N and, maturity T is

$$s(t,T) = -\frac{1}{T-t}\ln\left(\frac{B(t,T)}{N}\right) - r(t,T), \tag{2.1}$$

where $r(t,T)$ is the default-free spot rate prevailing at time t with maturity T.

2.1 Model 1

We first consider a bank with the liability side composed by deposits or, more generally, non-debt liabilities (*Ndl*), senior (*Sen*) and subordinated debt (*Sub*). Thus, the total market value of the liabilities is

$$L(t,T) = Ndl(t,T) + Sen(t,T) + Sub(t,T), \tag{2.2}$$

where $Ndl(t,T)$, $Sen(t,T)$ and $Sub(t,T)$ are the time t values of non-debt liabilities, senior and subordinated bonds with maturity T and face values N_{ndl}, N_{sen}, and N_{sub}, respectively. In equation (2.2) the claims are ranked by the order of priority of payments.

While collapsing debt on a single date is a restrictive assumption, it is an hypothesis underpinning the vast majority of structural credit risk models starting from the seminal works of Merton [1974] and Black and Cox [1976] up to more recent works, including the model of Hilscher and Raviv [2014], which we extend and calibrate on real data in this contribution.

It should be noted that non-debt liabilities represent a large portion of the liability side of a bank and a commercial bank usually relies on different funding sources. Non-debt liabilities include deposits, credit operations with the central bank and other banks, and derivatives. Even if there are more realistic models of the bank balance sheet structure (e.g. Li et al. [2018]), we consider a simplified model for the liability side where all non-debt liabilities are considered risk-free since our main purpose is the analysis of debt instruments. This is equivalent to assume that there is a guarantee on deposits and all other non-debt liabilities are fully collateralized. Default can occur either before time T, if the value of the assets falls below a threshold linked to the deposits amount, or at time T, if the bank assets value is smaller than the liabilities face value. Specifically, the default time is defined as

$$\tau = \inf\left\{t > 0 \middle| A_t \leq K_t\right\}, \tag{2.3}$$

where

$$K_t = \alpha_{ndl} N_{ndl}, \quad \forall t < T,$$

and

$$K_t = N_{ndl} + N_{sen} + N_{sub} = L, \quad t = T,$$

with α_{ndl} in the interval $[l_{\alpha_{ndl}}, u_{\alpha_{ndl}}]$, where $l_{\alpha_{ndl}}$ and $u_{\alpha_{ndl}}$ are two positive numbers close to 1.[2] The α_{ndl} parameter reflects the ability of the supervisory authority to monitor the bank activity and the willingness of the authority to take remedial actions:

[2]See Section 6.1 for a detailed discussion on the seleleciton of $l_{\alpha_{ndl}}$ and $u_{\alpha_{ndl}}$.

- $\alpha_{ndl} > 1$ implies a strong control by the supervisory authority, which is capable of imposing bankruptcy before the bank assets reach the value of the deposits;
- $\alpha_{ndl} = 1$ implies a perfect ability by the supervisory authority to take remedial actions as soon as the value of the assets equals the deposits;
- $\alpha_{ndl} < 1$ denotes less frequent or less rigid controls by the supervisors.

Furthermore, we assume that in case of default before maturity, if $\alpha_{ndl} > 1$, non-debt holders receive N_{ndl} at time T and the amount $(\alpha_{ndl} - 1)N_{ndl}$ is devoted to costs of early bankruptcy, while if $\alpha_{ndl} \leq 1$, a portion is still meant to recover early default costs and non-debt holders receive N_{ndl} thanks to bank guarantees. These assumptions imply that all non-debt liabilities are fully repaid and in case of default before maturity debt holders receive nothing. The payoffs at maturity T of various claims holders can be written as

$$\begin{aligned}
Ndl(T,T) &= N_{ndl}, \\
Sen(T,T) &= N_{sen} I_{(\tau \geq T, A_T \geq N_{ndl}+N_{sen})} + \max\big\{(A_T - N_{ndl}), 0\big\} I_{(\tau \geq T, N_{ndl}+N_{sen} > A_T \geq N_{ndl})}, \\
Sub(T,T) &= N_{sub} I_{(\tau \geq T, A_T \geq L)} + \max\big\{(A_T - N_{ndl} - N_{sen}), 0\big\} I_{(\tau \geq T, L > A_T \geq N_{ndl}+N_{sen})}, \\
E_T &= \max\big\{(A_T - L), 0\big\} I_{(\tau > T)},
\end{aligned} \tag{2.4}$$

where the first equality in equation (2.4) implies that non-debt liabilities are always paid in full.

Equation (2.3) can be viewed as the first passage time problem of a geometric Brownian motion, in this case the total asset value A_t, across the threshold K_t (see Hieber and Scherer [2012]). As observed by Hieber and Scherer [2012] and Kim [2019], different distributional assumptions for the driving process could be considered. Here, as already explained in Section 1, we want to keep the framework as simple as possible to get closed-form solutions.

Non-debt liabilities price can be written as

$$Ndl(t,T) = \mathrm{E}_t^Q\big[e^{-r(T-t)} N_{ndl}\big] = e^{-r(T-t)} N_{ndl}, \tag{2.5}$$

where E_t^Q denote the expectation, given the information available at time t, under the risk-neutral probability measure Q.

As observed by Hilscher and Raviv [2014], the payoff of different liabilities can be replicated using a combination of different barrier options and, assuming the existence of a constant risk-free rate, r, and that the firm asset value evolves according to a geometric Brownian motion, it is possible to price liabilities and equities using closed formulas.

In particular, following the Hilscher and Raviv [2014] idea, senior and subordinated debt payoff in equation (2.4) can be written as

$$\begin{aligned}
Sen(T,T) &= \big[\max\big\{(A_T - N_{ndl}), 0\big\} - \max\big\{(A_T - N_{ndl} - N_{sen}), 0\big\}\big]\, I_{(\tau \geq T)}, \\
Sub(T,T) &= \big[\max\big\{A_T - N_{ndl} - N_{sen}), 0\big\} - \max\big\{(A_T - L), 0\big\}\big]\, I_{(\tau \geq T)},
\end{aligned} \tag{2.6}$$

and, therefore, their prices are

$$\begin{aligned}
Sen(t,T) &= \mathrm{E}_t^Q\big[e^{-r(T-t)} Sen(T,T)\big] \\
&= CB_{t,T}^{dout}(\alpha_{ndl} N_{ndl}, N_{ndl}) - CB_{t,T}^{dout}(\alpha_{ndl} N_{ndl}, N_{ndl} + N_{sen}),
\end{aligned} \tag{2.7}$$

$$\begin{aligned} Sub(t,T) &= \mathrm{E}_t^Q\left[e^{-r(T-t)}Sub(T,T)\right] \\ &= CB_{t,T}^{dout}(\alpha_{ndl}N_{ndl}, N_{ndl}+N_{sen}) - CB_{t,T}^{dout}(\alpha_{ndl}N_{ndl}, L), \end{aligned} \tag{2.8}$$

where $CB_{t,T}^{dout}(K,N)$ is a down-and-out call option with threshold level K, strike N, and maturity T. Finally, the equity price can be computed as

$$\begin{aligned} E_t &= \mathrm{E}_t^Q\left[e^{-r(T-t)}\big(\max\left\{(A_T-L,0\right\}I_{\tau>T}\big)\right] \\ &= CB_{t,T}^{dout}(\alpha_{ndl}N_{ndl}, L). \end{aligned} \tag{2.9}$$

Assuming that equity volatility can be expressed as $\sigma_E E_t$ and taking into account that $E_t = f(A_t, \sigma_A)$, an application of Ito's lemma allows to write

$$\sigma_E E_t = \frac{dE_t}{dA_t} A_t \sigma_A, \tag{2.10}$$

where[3]

$$\frac{dE_t}{dA_t} = N(d_1) - \left(\frac{\alpha L}{A_t}\right)^{\frac{2r}{\sigma_A^2}} \left[\frac{e^{-r(T-t)}}{\alpha} N(d_8)\left(\frac{2r}{\sigma_A^2}-1\right) - \frac{2r}{\sigma_A^2}\frac{\alpha L N(d_7)}{A_t}\right].$$

Even if in most of the practical applications, A_t and E_t represent the market value of assets and equity, in Section 6 equation (2.10) is implemented on the basis of the book values of assets and equity. The same considerations are true also for the model in Section 2.2. This assumption affects the estimation of the equity volatility only (i.e. the left side panel in Figure 6). This choice is motivated by the fact that in Section 3, the model inputs are based on balance sheet data and it allows one to have a consistency between the models in Section 2 and that one in Section 3.

The hypothesis of the existence of a constant riskless interest rate is made to get a model which can be easily implemented due to the availability of closed formulas. Russo et al. [2020a] studied an intensity-based reduced-form framework to model the behavior of both risk-free interest rates and credit spreads, where the two sources of risk are correlated, and they derived closed formulas for the price of European options having as underlying defaultable bonds.

To get a more realistic model under the structural framework, it is possible to relax the assumption of a constant riskless interest rate by assuming that the instantaneous risk-free rate is stochastic and correlated with the total asset value process. The impact of the correlation between interest rate and firm value was considered by Longstaff and Schwartz [1995] in the context of a first passage time credit risk model, in which the firm value follows a geometric Brownian motion with constant volatility, and the short rate is modeled as a Vasicek process (see Vasicek [1977]). They found that as the correlation between the two processes increases, credit spreads become slightly bigger. In particular, when the correlation is positive, the covariance term is added to the total variance of changes in the asset value and small increments in both risk-neutral default probabilities and spreads are observed. Conversely, a negative correlation implies slightly smaller risk-neutral bankruptcy probabilities and spreads.

As observed by Leland and Toft [1996], the introduction of a stochastic default-free interest rate process has a relatively small effect on credit spreads, while significantly

[3] For more details see Appendix A.1.1.

complicating the analysis. For this reason, while the assumption of a constant risk-free rate may constitute a marginal limitation, this simplifying hypothesis will allow us to calibrate the model with undoubted advantages in terms of precision and computing time.

2.2 Model 2

Now, we add an additional layer into the liability structure of the bank described in Section 2.1, that is additional tier 1 instruments better known as contingent convertible bonds (CoCos). Therefore, the market value of total liabilities is defined as

$$L(t,T) = Ndl(t,T) + Sen(t,T) + Sub(t,T) + CoCo(t,T), \tag{2.11}$$

where $Ndl(t,T)$, $Sen(t,T)$, $Sub(t,T)$ and $CoCo(t,T)$ are the time t values of non-debt liabilities, senior, subordinated and CoCo bonds with maturity T and face values N_{ndl}, N_{sen}, N_{sub} and N_{coco}, respectively. In equation (2.11) the claims are ranked by the order of priority of payments. Again default can occur either before time T, if the value of the assets falls below the threshold $\alpha_{ndl}N_{ndl}$, or at time T, if the bank assets value is smaller than the liabilities face value, which is defined in this case as $L = N_{ndl}+N_{sen}+N_{sub}+N_{coco}$.

Assuming the existence of risk less asset providing a constant rate of return r, the risk-neutral firm's assets value dynamics is still an exponential Brownian motion with drift r and volatility σ_A and, from the properties of Brownian motion's first passage time through a deterministic barrier, the risk-neutral default probability can be computed as

$$\begin{aligned} p(t < \tau \leq T) = N&\left(\frac{\ln(\frac{\alpha_{ndl}N_{ndl}}{A_t}) - (r - \frac{1}{2}\sigma_A^2)(T-t)}{\sigma_A\sqrt{T-t}}\right) \\ &+ \left(\frac{\alpha_{ndl}N_{ndl}}{A_t}\right)^{2\frac{r-\frac{1}{2}\sigma_A^2}{\sigma_A^2}} N\left(\frac{\ln(\frac{\alpha_{ndl}N_{ndl}}{A_t}) + (r - \frac{1}{2}\sigma_A^2)(T-t)}{\sigma_A\sqrt{T-t}}\right). \end{aligned} \tag{2.12}$$

Then, we introduce another hitting time, to which we refer to as *CoCo time* as

$$\tau_{coco} = \inf\left\{t > 0 \middle| A_t \leq K_{coco}\right\}, \tag{2.13}$$

where

$$K_{coco} = (1+\omega)(N_{ndl} + N_{sen} + N_{sub} + N_{coco}) = (1+\omega)L,$$

with ω in the interval $[l_\omega, u_\omega]$, where $l_\omega < 0$ and $u_\omega > 0$. As observed by Hilscher and Raviv [2014], the ω parameters captures the distance between the conversion threshold and the book value of the debt. A smaller ω implies conversion at periods of higher leverage and higher probability of financial distress. A bigger ω captures conversion at periods of lower leverage and less likelihood of financial distress. Since balance sheet data are released quarterly and the exact value of the minimum capital requirement is even not disclosed, some adjustment is needed to deal with this uncertainty. Restrictions on the ω are also necessary to get reasonable CoCo trigger levels (see also Section 6.1). The relation between α_{nld} and ω is such that the following inequality is always satisfied

$$\tau_{coco} < \tau,$$

and an inferior limit of ω is necessary to ensure that this inequality holds.

Using the first passage time properties of a Brownian motion across a constant barrier, we get the risk-neutral *Coco trigger* probability

$$\begin{aligned} p(t<\tau\leq T) = N\left(\frac{\ln(\frac{(1+\omega)L}{A_t})-(r-\frac{1}{2}\sigma_A^2)(T-t)}{\sigma_A\sqrt{T-t}}\right) \\ +\left(\frac{(1+\omega)L}{A_t}\right)^{2\frac{r-\frac{1}{2}\sigma_A^2}{\sigma_A^2}} N\left(\frac{\ln(\frac{(1+\omega)L}{A_t})+(r-\frac{1}{2}\sigma_A^2)(T-t)}{\sigma_A\sqrt{T-t}}\right). \end{aligned} \tag{2.14}$$

The payoffs at maturity T of *Ndl*, *Sen*, and *Sub* holders can be written as in equation (2.4) and the payoffs of the remaining claims are

$$\begin{aligned} CoCo(T,T) &= N_{coco}I_{(\tau_{coco}>T)} + \gamma\max\big\{(A_T-N_{ndl}-N_{sen}-N_{sub}),0\big\}I_{(\tau_{coco}\leq T<\tau)}, \\ E_T &= \max\big\{(A_T-N_{ndl}-N_{sen}-N_{sub}-N_{coco}),0\big\}I_{(\tau_{coco}>T)} \\ &\quad +(1-\gamma)\max\big\{(A_T-N_{ndl}-N_{sen}-N_{sub}),0\big\}I_{(\tau_{coco}<T<\tau)}, \end{aligned} \tag{2.15}$$

where γ is the conversion rate. If γ is equal to 0, then CoCo bonds are written down. Even if here we consider the more general case, in the empirical analysis in Section 6 we will always assume γ equal to 0.

Following Hilscher and Raviv [2014], the value at time t of each liability can be obtained by pricing a portfolio made up by a combination of barrier options replicating the payoffs in equations (2.4) and (2.15). Thus, it follows that the prices of non-debt liabilities, senior and subordinated bonds can be written as in equations (2.5), (2.7), (2.8). Then, the CoCo price is given by

$$\begin{aligned} CoCo(t,T) &= \mathrm{E}_t^Q\big[e^{-r(T-t)}Coco(T,T)\big] \\ &= N_{coco}DB_{t,T}^{dout}(K_{coco}) \\ &\quad +\gamma\big[CB_{t,T}^{din}(K_{coco},N_{ndl}+N_{sen}+N_{sub}) \\ &\quad -CB_{t,T}^{din}(\alpha_{ndl}N_{ndl},N_{ndl}+N_{sen}+N_{sub})\big], \end{aligned} \tag{2.16}$$

and the equity value is

$$\begin{aligned} E_t &= \mathrm{E}_t^Q\big[e^{-r(T-t)}E_T\big] \\ &= CB_{t,T}^{dout}(K_{coco},N_{ndl}+N_{sen}+N_{sub}+N_{coco}) \\ &\quad +(1-\gamma)\big[CB_{t,T}^{din}(K_{coco},N_{ndl}+N_{sen}+N_{sub}) \\ &\quad -CB_{t,T}^{din}(\alpha_{ndl}N_{ndl},N_{ndl}+N_{sen}+N_{sub})\big], \end{aligned} \tag{2.17}$$

where

- $CB_{t,T}^{dout}(K,N)$ is the price of a down-and-out barrier call option with threshold level K, strike N, and maturity T;
- $DB_{t,T}^{dout}(K)$ is the price of a down-and-out digital barrier option with a barrier K and maturity T;

- $CB^{din}_{t,T}(K,N)$ is the price of a down-and-in barrier call option with threshold level K, strike N and maturity T.[4]

Then, the equity volatility can be computed through equation (2.10) and the formula in the Appendix A.1.2.

3 Implied CET1 volatility

The common equity tier 1 (CET1) ratio is defined as the ratio between common equity tier 1 and risk weighted assets (RWA). Extending the model first analyzed by De Spiegeleer et al. [2017], and further investigated by Choe et al. [2019], we consider a CoCo bond as a contract written on the CET1 ratio. Then, we describe the dynamics of this ratio as a geometric Brownian motion and we apply a pricing methodology based on a hitting time probability similar to that described in Section 2. An analogue approach has been recently proposed by Russo et al. [2020b]. While De Spiegeleer et al. [2017] specified directly the risk-neutral dynamics of the CET1 ratio as a geometric Brownian motion with zero drift, Choe et al. [2019] defined its dynamics as the ratio of two correlated Brownian motions.

Similarly to Choe et al. [2019], we describe the evolution of the CET1 ratio by modeling the bank assets and equity as two correlated processes without looking at the equity as an option written on the assets (differently with respect to Section 2). This approach allows to calibrate the two marginal processes and the dependence structure separately. In particular, assuming that both A_t and E_t are dependent geometric Brownian motions, A_t and E_t can be calibrated by considering bond spreads or (and) equity implied volatilities, respectively, the correlation parameter gives an additional degree of freedom useful to calibrate the observed CoCo spreads.

As shown in details in Appendix A.2, we obtain the CET1 dynamics by modeling the equity and the asset of the CET1 ratio as two correlated geometric Brownian motions. The market value of the CET1 ratio can be defined as the process

$$CET1_t = \frac{E_t}{wA_t}, \tag{3.1}$$

where w is the risk density. The risk density is defined as the ratio between RWA to total asset and it is a constant observed at time t.

Under these assumptions, it can be shown that under the risk-neutral measure the CET1 ratio is a geometric Brownian motion, that is

$$\frac{dCET1_t}{CET1_t} = \mu_{CET1}dt + \sigma_{CET1}dW_t, \tag{3.2}$$

where μ_{CET1} and σ_{CET1} are functions of asset and equity volatilities and of their correlation ρ (see Appendix A.2). Thus, we define the following hitting time

$$\tau_{cet1} = \inf\left\{t > 0 \middle| CET_t \leq Trigger\right\}, \tag{3.3}$$

[4] A review of barrier options pricing formulas in the context of Black and Scholes assumptions is provided in the Appendix of Hilscher and Raviv [2014].

and the probability that the CET1 ratio hits the trigger level is given by

$$p(t < \tau_{cet1} \leq T) = N\left(\frac{\ln(\frac{Trigger}{CET1_t}) - (\mu_{CET1} - \frac{1}{2}\sigma^2_{CET1})(T-t)}{\sigma_{CET1}\sqrt{T-t}}\right) + \left(\frac{Trigger}{CET1_t}\right)^{2\frac{\mu_{CET1}-\frac{1}{2}\sigma^2_{CET1}}{\sigma^2_{CET1}}} N\left(\frac{\ln(\frac{Trigger}{CET1_t}) + (\mu_{CET1} - \frac{1}{2}\sigma^2_{CET1})(T-t)}{\sigma_{CET1}\sqrt{T-t}}\right). \tag{3.4}$$

The formula (3.4) was originally proposed by De Spiegeleer et al. [2017], but it can be also obtained by calibrating the two components of the ratio. This means that it is possible to calibrate the model on observed CoCo spreads only, as studied in De Spiegeleer et al. [2017], or on asset and equity implied volatilities extracted from senior, subordinated, and CoCo spreads (or option data) simultaneously under the unified framework briefly described here and in Section 2 (see Section 4 and the Appendix A.2 for further details). Using this second calibration approach, one approximates the equity dynamics in equation (2.17) as a geometric Brownian motion.

The bond spread can be computed through the following equation

$$s(t,T) = -\frac{\log(1-(1-\gamma)\,p(t < \tau_{cet1} \leq T))}{T-t}, \tag{3.5}$$

where γ is the recovery rate. If the CoCo bond is written down in case the trigger event occurs, it has a zero recovery rate (i.e. $\gamma = 0$).

As observed above, if we assume $\mu_{CET1} = 0$ as in De Spiegeleer et al. [2017], the parameter σ_{CET1} can be estimated by assuming a dynamics as in equation (3.2) and can be extracted from CoCo spreads, that is at each given trading date, after having defined a proper trigger and starting from the spread, it is possible to determine σ_{CET1}. This is the reason why we refer to σ_{CET1} as *implied CET1 ratio volatility*. This implied volatility reflects the view of the market on the dynamics of the CET1 ratio under the assumption of equation (3.2). It appears clear that one of the main parameters is the trigger level. A possible choice is described in Section 5.

4 Asset, equity and CET1 ratio volatilities

Now, we are in the position to analyze the relation between three implied volatilities: asset volatility, equity volatility and CET1 ratio volatility. In particular, we want to verify if the implied volatilities, σ_A and σ_E, estimated by calibrating the model described in Section 2.2, can be used as input for the pricing of CoCo bonds, according to the formulas provided in Section 3 and in the Appendix A.2. This would allow us to extend the model defined in Sections 2.2 to calibrate observed market prices under a comprehensive approach linking asset, equity and CET1 ratio volatilities.

Even if it is possible to calibrate the implied CET1 volatility directly from observed CoCo spreads (see De Spiegeleer et al. [2017]), we propose here a different approach relying on a structural model. On the basis of observed spreads and balance sheet information, we

calibrate all parameters of the model defined in Section 2.2 and, after setting a regulatory trigger level, we assume that

$$p(t < \tau_{cet1} \leq T) = p(t < \tau_{coco} \leq T), \tag{4.1}$$

where, as originally proposed by De Spiegeleer et al. [2017], the CET1 ratio process is a geometric Brownian motion obtained as the ratio in equation (3.2) in which two dependent geometric Brownian motions are taken into account (i.e. E_t and A_t). Equation (4.1) allows us to connect the structural approach described in Section 2.2 with the one consisting in modeling the dynamics of the CET1 ratio. Therefore, after calibrating the structural model, it is possible to extract the CET1 ratio volatility.

Additionally, under the bivariate approach proposed in Section 3, we are implicitly assuming that the CET1 volatility is also given by

$$\sigma_{CET1} = \sqrt{\sigma_A^2 + \sigma_E^2 - 2\rho\sigma_A\sigma_E}, \tag{4.2}$$

where ρ is the equity and asset return correlation. After calibrating the three volatilities, σ_A, σ_E and σ_{CET1}, it is possible to obtain, by means of the equality (4.2), an estimate of the ρ (see Appendix A.2, where the formula for the drift μ_{CET1} is also provided).

Unfortunately, as discussed in Section 6.2, if one considers both σ_A and σ_E extracted from senior and subordinated bonds, is not possible to find a ρ satisfying the equality (4.2). For this reason, we implement the following approach: (1) by the model in Section 2.2, we extract σ_A (and σ_E) from senior, subordinated and CoCo bonds; (2) we link, through equation (4.1), the structural model in Section 2.2 and the bivariate geometric Brownian motion of E_t and A_t driving the dynamics of the CET1 ratio; (3) we obtain an estimate for σ_E and ρ from equation (4.2). The estimate of σ_E obtained in step (1) is the starting point for the estimation conducted in step (3).

As already observed in Section 3, the models proposed in Sections 2.2 and 3 are not theoretically coherent. While in the model described in Section 2.2 the equity is defined as an option written on the bank asset, in the model described in Section 3 the equity is defined as a geometric Brownian motion. From one side, we assume that E_t is given by equation (2.17), from the other side, we assume that E_t is a geometric Brownian motion. However, this approximation seems acceptable, mainly because one considers only the volatilities of the driving processes. Furthermore, it is a common practice in implementation of structural models to extract asset volatility from equity volatility implicitly relying on the assumption that equity follows a geometric Brownian motion or, more generally, that equity volatility can be expressed as $\sigma_E E_t$, and then by applying Ito's lemma to the equity price function $E_t = f(A_t, \sigma_A)$.

5 Data

We distinguish between four different sets of data: (a) financial instrument characteristics; (b) bond and credit default swap market data; (c) bank balance sheet and capital data; (d) minimum capital requirements.

Financial instrument characteristics (i.e. security type, issuer sector, issuer country or region, issue date, early redemption date, maturity, and currency) are extracted by

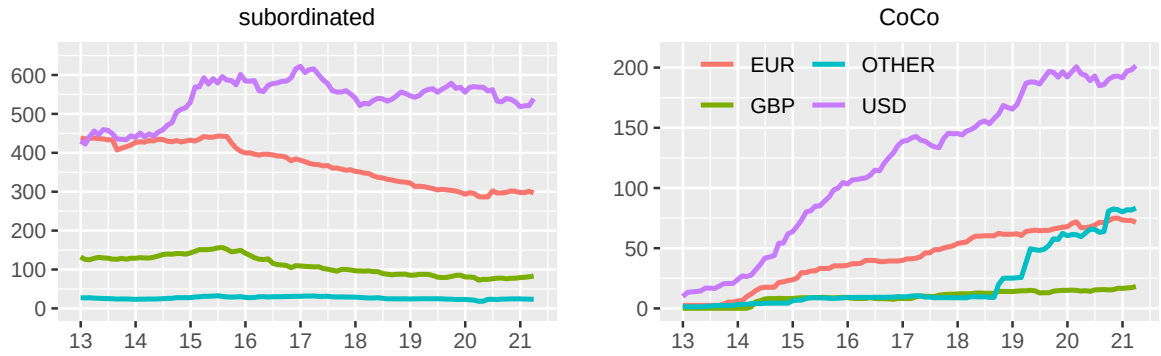

Figure 1: Subordinated and CoCo bonds outstanding volume in billion euro from December 2012 to March 2021 for banks and other financial institutions. We consider all bonds issued in euro, sterling, US dollar and other currencies (other) and all volumes are reported in euro.

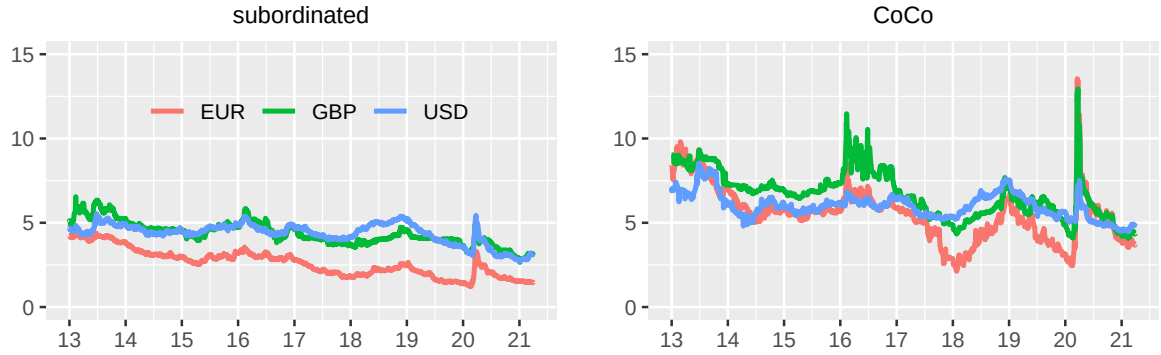

Figure 2: Subordinated and CoCo bonds yield in percentage points from December 2012 to March 2021 for banks and other financial institutions for different currencies. We consider all bonds issued in euro, sterling and US dollar.

the Securities Database (Anagrafe Titoli[5]) managed by the Banca d'Italia and combined with additional information obtained through Refinitiv (i.e. next call date for AT1 bonds and total market outstanding and early redemption date for all subordinated and AT1 bonds). The Securities Database contains the details of financial instruments outstanding in Italy or those that supervised intermediaries and other companies report to the Banca d'Italia, including most of the bonds issued by European and non-European banks and financial institutions. On the basis of the information stored in this database, we select a sample of subordinated and AT1 bonds issued by banks and other financial institutions in the period from December 31, 2012 to March 31, 2021. For each ISIN we extract the bond characteristics.

Before focusing on the sample used in the empirical analysis, we provide a general overview on the market of subordinated and AT1 bonds. To this aim we deal with 4,887

[5] The ISIN code of the securities and some related information are publicly available on the Banca d'Italia website.

debt securities (4,353 subordinated bonds and 534 AT1 bonds) issued by European and non-European banks and other financial institutions. We consider all debt securities collected in the Securities Database, which are a representative sample of global outstanding subordinated and AT1 bonds. In Figure 1 we report the total outstanding volume for all bonds for which data are available in Refinitiv. While the growth of CoCo bonds in euro, sterling and US dollar, is mainly motivated by the entering into force of the CRD IV package in 2014, the growth observed in outstanding volume in *other* currencies is due to the issues of Chinese commercial banks in the last years (see Li et al. [2020]). Then, we select 153 issuers for which both subordinated and AT1 bonds are available for a total of 1,857 bonds. In Figure 2 we show the daily historical evolution of the median annual yield reported in Refinitiv for all bonds issued in euro, sterling and US dollar by the 153 issuers of the selected sample.

For the empirical analysis conducted in Section 6, we select a sample of 20 euro area banks.[6] All market data (e.g. bond yields) are extracted from Refinitiv. As far as bank data are concerned, total assets, total liabilities, total subordinated debt, common equity tier 1 and risk weighted assets are downloaded from the S&P Global Market Intelligence platform from each quarter from December 31, 2012 to December 31, 2020. Balance sheet and capital data are considered only for these 20 banks. This data are inputs for the formulas described in Section 2. Thus, we analyzed 659 bonds (537 subordinated bonds and 122 CoCo bonds) issued by these banks and outstanding from December 31, 2012 to March 31, 2021. In order to easily compare the risk of different banks, we consider the senior and subordinated CDS spreads with maturity between 1 year and 10 years. A structural break is observed at the end of 2014 when the ISDA 2014 credit event definition was adopted (Neuberg et al. [2016]). All spreads are downloaded through DSWS and the source of these CDS data is Credit Market Analysis (CMA). Then, we obtain from DSWS the implied volatilities extracted from European call and put options written on the selected stocks with five year maturity and with moneyness equal to 100% (i.e. at-the-money). Additionally, to estimate euro denominated 5-year spreads, we also download euro, sterling and US dollar interest rate swap and euro and sterling currency basis swap data with maturities from one to 30 years.

In this paper, a breach of a CoCo bond occurs when the CET1 process falls below the CET1 requirement. Minimum capital requirements have changed over time and across banks and they reflect not only the risk of a given bank but also the evolution of prudential rules (see Bevilacqua et al. [2019] and Dautović [2020]). According to the data reported on the Supervisory review (SREP) pages of the European Central Bank website, for the banks supervised through the Single Supervisory Mechanism (SSM) the average CET1 requirement increases from 10.2% in 2016 to 10.5% in 2021. It was 9% in 2012, according to the European Banking Authority [2012] recommendation. In the empirical analysis we will not consider the non-binding Pillar 2 Guidance (P2G) component of the requirement and for all banks the trigger will be the average CET1 requirement minus

[6] The banks in the sample are: ABN AMRO Bank (H:ABN), Banco Bilbao Vizcaya Argentaria (E:BBVA), Banco BPM (I:BP), Banco Sabadell (E:BSAB), Banco Santander (E:SAN), Bankia (E:BKIA), Bankinter (E:BKT), BNP Paribas (F:BNP), Caixabank (E:CABK), Commerzbank (D:CBK), Crédit Agricole (F:CRDA), Deutsche Bank (D:DBK), Erste Group Bank (O:ERS), ING Groep (H:INGA), Intesa Sanpaolo (I:ISP), KBC Group (B:KB), Nordea Bank (M:NBH), Raiffeisen Bank International (O:RAI), Société générale (F:SGE), Unicredit (I:UCG), Unione di Banche Italiane (I:UBI). In April 2021 I:UBI was incorporated into I:ISP.

the P2G component (i.e. from 7.9 in 2013 to 8.9 in 2021). The P2G for years from 2013 to 2015 is estimated on the basis of the average P2G applied from 2016 to 2021. All data are public available.

Since it is not simple to find publicly available data on the requirements related to each single bank in the sample and over the entire observation window from 2013 to 2021, we do not consider the bank specific capital requirements but the average value based on the sample of all banks supervised by SSM. This seems a reasonable assumption since in the empirical analysis we study the main European banks supervised by the SSM. Note that the trigger parameter is needed in equations (3.3) and (4.1) in Sections 3 and 4, respectively, but it does not enter into the model studied in Section 2.2. In comparison with De Spiegeleer et al. [2017], even if we assume the same trigger for all banks in the sample, its level in our empirical study is always higher and it varies across different years.

6 Empirical analysis

Before starting the empirical analysis, on the basis of quoted yields and subordinated CDS curve, we extract the euro denominated 5-year spreads for all subordinated and CoCo bond issued by the selected euro area banks. These spreads are obtained by considering for each currency the reference interest rate swap curve and, for all US dollar and sterling denominated bonds, the currency basis swap curve. In the evaluation of the spread, a linear interpolation approach is applied to deal with the residual maturity of the bonds. These spreads are computed by taking into account, for each given trading day, the median difference between the spread of the subordinated (CoCo) bond with respect the subordinated CDS curve of the issuer. These median differences are then added to the observed 5-year subordinated CDS spread to obtained the 5-year subordinated (CoCo) bond spread. For all selected banks we have senior and subordinated CDS spreads, and subordinated and CoCo bonds spreads, with the same maturity, i.e. 5 years. Senior, subordinated and CoCo spreads are the inputs for the model calibration described in Section 6.1.

In Figure 3 we report the average values of the spread over the entire observation window. There are some differences between subordinated CDS spreads and the spreads extracted from subordinated bonds, mainly before 2015. For less recent trading days and for some banks, the quality of the spreads is poor, mainly because the quality of the input data is not always adequate. Also for this reason, the time-series of the estimated parameters might present some outliers. Since in most of the cases the spreads extracted from subordinated bonds seem more reliable (i.e. they show a larger difference with respect to senior spreads), we consider them in the empirical analysis.

6.1 Calibration results

The calibration is conducted for each trading day from December 31, 2012 to March 31, 2021. For each bank i, on each trading day t, we estimate the model parameters by

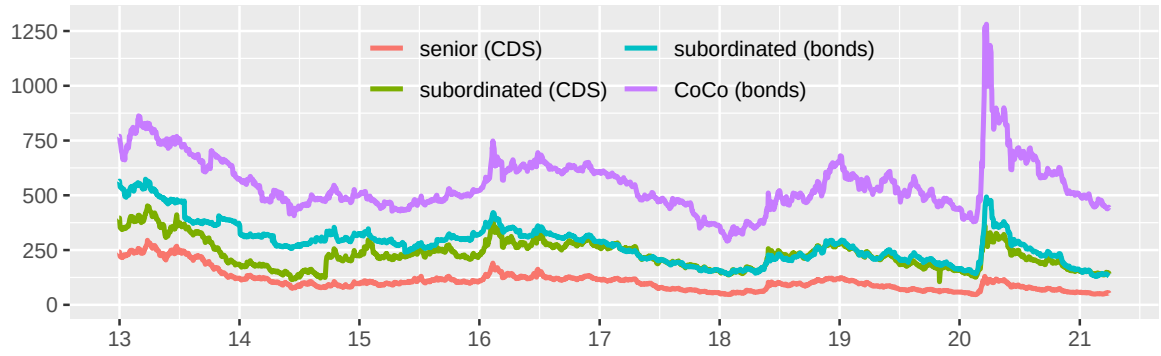

Figure 3: CDS and bond credit spreads in basis points from December 2012 to March 2021 for the selected European banks in the sample. We report the average values across the entire sample.

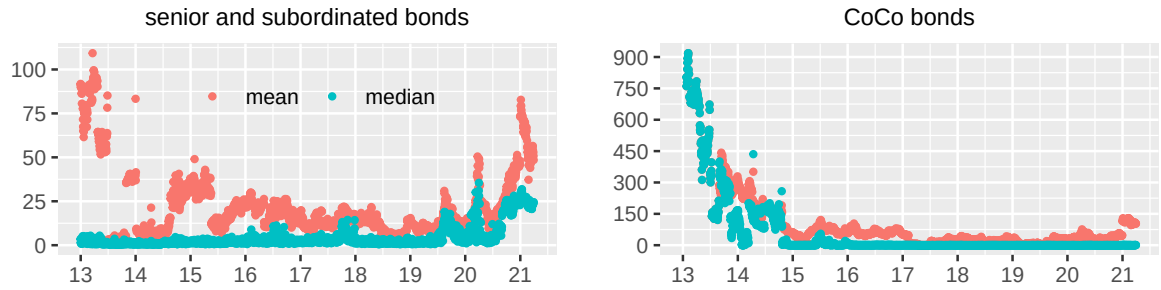

Figure 4: Basis points calibration error on senior and subordinated bond spreads ($error_1$) and on CoCo bond spreads ($error_2$) from December 2012 to March 2021 for the European banks in the sample. We report the mean and the median values across the entire sample.

solving the following minimization problem

$$\widehat{\Theta}^{Q_t^i} = \min_{\Theta^{Q_t^i}} \left(\sum_j \left(spread_{j,t}^{market} - spread_{j,t}^{model}(\Theta^{Q_t^i}) \right)^2 \right)^{\frac{1}{2}}, \tag{6.1}$$

in which $spread_{j,t}^{market}$ ($spread_{j,t}^{model}$) denotes the market (model) spreads, the index j represents the bond type j, and $\Theta^{Q_t^i}$ is the vector of the risk-neutral parameters at time t. This means in practice that for each bank we consider at most 2,153 different trading days and calibrations. There are two possible alternatives: (1) one can, first, calibrate the parameters σ_A and α_{ndl} to senior and subordinated bonds and, then, the parameter ω to CoCo spreads; (2) one can jointly calibrate all parameters, that is σ_A, α_{ndl} and ω, to the three different types of bonds. Since CoCo spreads data are not always available, in order to have a longer time-series of σ_A estimates, we select the first approach. Therefore, for each bank and each trading day, we solve two optimization problems.

The model is calibrated under a static perspective, that is at each given point in time model prices have to be as close as possible to the prices traded in the market. Whatever the market prices are, we find the parameters trying to replicate those prices. As explained by Nawalkha and Rebonato [2011], this approach is usually implemented

bank	$error_1$						$error_2$						$nobs_1$	$nobs_2$
	min	q_{25}	q_{50}	mean	q_{75}	max	min	q_{25}	q_{50}	mean	q_{75}	max		
D:bank1	0.001	0.156	0.691	5.253	3.218	69.427	0.069	437.744	497.516	481.453	563.285	720.172	1305	393
D:bank2	0.097	1.885	3.885	16.497	14.270	101.375	0.000	0.504	1.629	41.618	57.465	834.824	2153	1790
E:bank1	0.003	0.273	1.194	7.040	12.472	65.910	0.000	0.078	0.153	31.880	0.245	792.609	2153	2017
E:bank2	0.001	0.342	1.226	34.628	6.168	1346.105	0.000	0.067	0.223	14.533	0.271	483.810	2153	1018
E:bank3	0.010	0.532	1.437	9.636	4.571	101.753	0.000	0.087	0.123	27.638	0.285	586.079	2153	1953
E:bank4	0.001	20.525	45.407	139.890	97.956	1221.047	0.000	0.298	0.944	163.190	223.847	1284.786	1893	974
E:bank5	0.005	0.499	1.413	5.719	3.660	92.988	0.018	0.652	1.125	1.191	1.334	10.206	2153	146
F:bank1	0.014	0.616	3.368	23.030	36.403	228.671	0.000	0.135	0.449	16.210	1.404	264.700	2153	1513
F:bank2	0.032	1.101	3.819	23.577	26.119	256.856	0.000	0.501	0.692	122.426	65.521	1100.220	2153	1969
F:bank3	0.011	1.260	2.903	11.720	21.457	87.129	0.000	0.430	0.583	26.320	1.052	487.132	2153	1979
H:bank1	0.012	0.953	1.773	7.641	4.004	69.798	0.000	0.247	0.384	1.118	0.604	65.777	2036	1446
H:bank2	0.000	0.143	2.222	10.291	19.586	74.456	0.000	0.184	0.475	182.207	502.454	711.223	1501	1429
I:bank1	0.005	0.169	0.434	2.876	2.074	133.477	0.001	0.260	0.327	4.855	0.489	149.768	848	513
I:bank2	0.006	0.448	0.827	1.576	1.849	20.095	0.000	0.203	0.262	11.469	0.377	217.536	2153	1436
I:bank3	0.005	0.279	0.641	1.735	1.608	107.128	0.000	0.254	25.965	55.412	100.605	333.654	2153	1763
I:bank4	0.005	0.393	0.830	4.375	2.583	181.242	0.001	0.063	0.081	18.159	0.362	203.198	2153	219
O:bank1	0.004	0.193	0.833	3.894	5.013	44.703	0.000	0.198	0.273	23.158	45.732	132.513	2153	1264
O:bank2	0.008	8.569	25.805	46.495	64.751	444.615	0.000	0.148	0.199	12.696	1.073	128.927	2153	977
bank19	0.026	5.256	37.384	43.227	60.041	373.640	0.000	0.137	0.220	57.255	25.300	918.397	2153	1854
bank20	0.022	2.186	24.425	25.585	40.393	96.485	0.000	0.235	0.437	2.930	0.671	349.943	2153	1671
total	0.000	0.568	2.233	21.620	20.946	1346.105	0.000	0.172	0.410	53.522	5.660	1284.786	39878	26324

Table 1: Calibration errors on senior and subordinated bond spreads ($error_1$) and on CoCo bond spreads ($error_2$) from December 2012 to March 2021 for all European banks in the sample. The error measure is defined in equation (6.1) as the square root of the sum of the squares of the differences between observed and model spreads. Summary statistics: minimum, 0.25-quantile (q_{25}), median (q_{50}), mean, 0.75-quantile (q_{25}), and maximum over the entire observation window. We report the number of observations for senior and subordinated bonds ($nobs_1$) and for CoCo bonds ($nobs_2$).

bank	σ_A						α_{ndl}						ω						$nobs_1$	$nobs_2$
	min	q_{25}	q_{50}	mean	q_{75}	max	min	q_{25}	q_{50}	mean	q_{75}	max	min	q_{25}	q_{50}	mean	q_{75}	max		
D:bank1	0.022	0.029	0.033	0.036	0.043	0.061	0.857	0.960	1.004	0.975	1.009	1.059	-0.005	-0.005	-0.004	-0.003	-0.002	0.018	1305	393
D:bank2	0.011	0.019	0.024	0.023	0.027	0.046	0.937	1.103	1.148	1.142	1.196	1.249	-0.014	-0.012	-0.010	-0.009	-0.006	-0.000	2153	1790
E:bank1	0.017	0.031	0.036	0.039	0.041	0.088	0.848	0.848	1.001	0.948	1.008	1.030	-0.027	-0.013	-0.002	-0.001	0.010	0.047	2153	2017
E:bank2	0.010	0.033	0.042	0.048	0.059	0.121	0.903	1.004	1.044	1.031	1.070	1.165	-0.018	-0.007	-0.003	0.005	0.012	0.050	2153	1018
E:bank3	0.013	0.028	0.033	0.034	0.037	0.074	0.928	1.047	1.080	1.065	1.100	1.163	-0.017	-0.005	0.000	0.002	0.010	0.045	2153	1953
E:bank4	0.010	0.030	0.038	0.044	0.042	0.186	0.850	0.853	0.855	0.878	0.864	1.018	-0.016	-0.013	-0.009	-0.002	0.002	0.050	1893	974
E:bank5	0.013	0.023	0.029	0.032	0.036	0.077	0.856	1.013	1.055	1.050	1.100	1.151	-0.009	-0.004	-0.002	-0.002	-0.001	0.004	2153	146
F:bank1	0.010	0.019	0.023	0.027	0.039	0.059	0.986	1.102	1.134	1.130	1.181	1.284	-0.013	-0.007	-0.002	0.000	0.003	0.050	2153	1513
F:bank2	0.010	0.016	0.020	0.022	0.026	0.049	1.024	1.048	1.074	1.089	1.134	1.176	-0.022	-0.018	-0.013	-0.012	-0.006	0.005	2153	1969
F:bank3	0.010	0.019	0.022	0.023	0.025	0.049	1.015	1.150	1.211	1.215	1.301	1.346	-0.018	-0.011	-0.007	-0.008	-0.004	0.002	2153	1979
H:bank1	0.011	0.019	0.022	0.023	0.025	0.047	1.114	1.238	1.273	1.263	1.296	1.394	-0.033	-0.015	-0.012	-0.012	-0.007	-0.000	2036	1446
H:bank2	0.010	0.016	0.022	0.023	0.030	0.039	0.890	0.995	1.025	1.027	1.075	1.139	-0.022	-0.018	-0.003	-0.004	0.003	0.044	1501	1429
I:bank1	0.021	0.031	0.038	0.039	0.048	0.065	0.866	1.006	1.011	1.006	1.020	1.047	-0.022	-0.017	-0.013	-0.012	-0.007	0.023	848	513
I:bank2	0.020	0.030	0.035	0.037	0.040	0.076	0.997	1.026	1.049	1.076	1.115	1.232	-0.027	-0.021	-0.016	-0.016	-0.012	0.007	2153	1436
I:bank3	0.020	0.033	0.037	0.040	0.042	0.073	0.878	1.026	1.058	1.052	1.075	1.124	-0.027	-0.024	-0.022	-0.020	-0.018	0.010	2153	1763
I:bank4	0.012	0.037	0.048	0.046	0.056	0.078	0.943	1.119	1.206	1.223	1.360	1.443	-0.021	-0.015	0.003	-0.003	0.007	0.013	2153	219
O:bank1	0.026	0.036	0.039	0.043	0.046	0.075	0.874	0.883	1.005	0.971	1.017	1.058	-0.035	-0.032	-0.029	-0.022	-0.009	0.017	2153	1264
O:bank2	0.010	0.041	0.050	0.054	0.068	0.107	0.825	0.842	0.862	0.877	0.879	1.005	-0.050	-0.032	-0.018	-0.021	-0.011	0.041	2153	977
bank19	0.010	0.021	0.031	0.032	0.039	0.091	0.851	0.880	0.905	0.940	0.986	1.120	-0.044	-0.022	-0.010	-0.004	0.023	0.047	2153	1854
bank20	0.011	0.016	0.020	0.021	0.023	0.040	1.201	1.256	1.312	1.321	1.359	1.536	-0.020	-0.007	-0.004	-0.004	-0.001	0.019	2153	1671

Table 2: Estimated parameters from December 2012 to March 2021 for all European banks in the sample. Summary statistics: minimum, 0.25-quantile (q_{25}), median (q_{50}), mean, 0.75-quantile (q_{25}), and maximum over the entire observation window. We report the number of observations for senior and subordinated bonds ($nobs_1$) and for CoCo bonds ($nobs_2$).

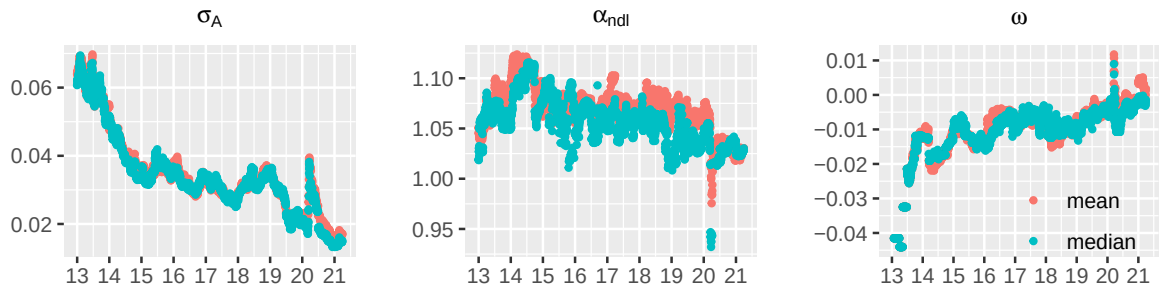

Figure 5: Estimated parameters from December 2012 to March 2021 for the European banks in the sample. We report the mean and the median values across the entire sample.

by traders and risk managers to achieve static consistency in order to provide at each given point in time arbitrage-free prices or to hedge a derivatives portfolio.

In Tables 1 and 2 we report the summary statistics of the calibration errors and of the estimated parameters. The error measure is defined in equation (6.1) as the square root of the sum of the squares of the differences between observed and model spreads.

Figure 4 shows the dynamics of the calibration error over time. As observed above, the quality of the market data is not always satisfactory, particularly for some banks and before 2014, when the outstanding amount of CoCo bonds was a few billions euro. As shown in Figure 4, the time series of the median error for senior and subordinated bonds computed across all 20 banks ranges from 0.30 to 35.47 basis points (on average, 4.36 basis points). By looking at the median error, as expected, on March 2020 the model reaches the largest calibration error. Since the median (mean) calibration error over time and across the sample of the selected European banks (around 40,000 observations) is 2.23 (21.62) basis points, we can conclude that the structural model is able to reproduce the spreads of senior and subordinated bonds observed in the market. We reach the same conclusion also in the CoCo bond case: the overall median (mean) calibration error is 0.41 (53.52) basis points (around 26,000 observations). For the three types of bonds analyzed here, the calibration error remains at acceptable levels. This empirical finding confirms that our model works properly.

To solve the optimization problem in equation (6.1), we consider the *optimx* function in R with the L-BFGS-B option. To obtain a satisfactory calibration to observed spreads and to be sure to have always proper barrier levels (i.e. the barrier should be always well below the total assets value), the lower and upper bounds of the parameters α_{ndl} and ω are selected on each time t. On the basis on balance sheet data observed at time t, we introduce the constants

$$
\begin{aligned}
c_1 &= \frac{N_{ndl} + N_{sen} + N_{sub}}{N_{ndl}}, \\
c_2 &= \frac{TotalAssets}{N_{ndl}}, \\
c_3 &= \min(0.95c_1, 0.9c_2),
\end{aligned}
$$

where $TotalAssets$ are the balance sheet total assets, and we compute the lower and the

upper bound of the parameter α_{ndl} as

$$u_{\alpha_{ndl}} = c_3,$$
$$l_{\alpha_{ndl}} = 0.8c_3.$$

Similarly, we compute the lower bound of the parameter ω as

$$l_\omega = \max(0.99c_4, -0.05),$$

where

$$c_4 = \frac{N_{ndl} + N_{sen}}{N_{ndl} + N_{sen} + N_{sub} + N_{coco}} - 1,$$

and u_ω is equal to 0.05. After some attempts, these bounds have been set to avoid unusual dynamics of estimates or unreasonable barrier levels. Given our static perspective, this can be viewed as a compromise providing a less robust calibration compared to a more complex approach. This allows one to obtain estimates having a meaning under financial and balance sheet perspectives. Figure 5 shows the dynamics of the estimated parameters over time. There are not material differences between average and median values.

Even with some exceptions, the parameter α_{ndl} is very close to 1, and in most of the cases, the parameter ω is slightly negative, even if it is on average close to 0 (see Table 2). The other parameter (i.e. σ_A), which is the most important in our analysis, shows a smoother dynamics over time. In the optimization algorithm, we constrain this parameter in the region between 0.01 and 0.25. Both balance sheet data and observed spreads may affect the stability of the estimated parameters over time. Since balance sheet data are released on a quarterly basis, these data are not as smooth as daily data. As described by Derksen et al. [2018], there is an *accounting noise* due to the fact that market participants get only imperfect information about the underlying asset dynamics through noisy accounting reports, issued at regular discretely spaced time points.

6.2 Implied volatilities dynamics

In this section we study the dynamics of the estimated implied volatilities. As already observed, there are various model dependent volatilities that can be extracted from different market spreads or quotes. Even if implied volatility estimates are available for all banks in the sample, we analyze their historical evolution only for the subsample of banks with the parent company domiciled in Germany, Spain, France and Italy. In addition, for each of these countries we represent weighted historical implied volatilities obtained by using the bank's total assets as weights of each bank's specific volatility.

After estimating the model parameters as described in Section 6.1, the implied equity volatility can be computed as shown in Section 2 (the relevant formulas are provided in the Appendix A.1). This implied equity volatility is extracted from credit market quotes and may differ from the implied equity volatility extracted from equity option data. Then, from the equality (4.1) the CET1 ratio volatility can be obtained. Thus, in theory, given the risk density and the estimates of three volatilities (i.e. asset, equity and CET1) it is possible to extract the correlation ρ between asset and equity. This estimate is derived from credit market quotes as well.

Unfortunately, if one considers the equity volatility extracted from senior and subordinated bonds, we cannot find a correlation ρ satisfying the equality (4.1). This is

mainly due to the fact that the estimated implied equity volatility extracted from senior and subordinated bonds is usually too high to obtain a proper CET1 ratio volatility. By equation (A.5), if the equity volatility is high, the CET1 volatility is also high. For this reason, in equality (4.1) and formulas (A.4), (A.5) and (A.6), we fix only the asset volatility σ_A to the value obtained in Section 6.1, and then we calibrate both ρ and σ_E. The optimization problem to solve is the minimization of the absolute value of the differences between the two probabilities $p(t < \tau_{coco} \leq T)$ and $p(t < \tau_{cet1} \leq T)$: the former given by the structural model in Section 2.2, the latter given by the CET1 ratio dynamics in Section 3. Also in this case we consider the *optimx* function in R with the L-BFGS-B option. We constrain the parameter ρ in the region between 0 and 0.8, and σ_E in the region 0.05 and 0.25.

This approach allows us to compare the equity volatility estimated through the structural approach to the equity volatility obtained by modeling the CET1 ratio dynamics. We deal with three different implied equity volatilities coming from: (1) the structural model; (2) CET1 ratio volatility; (3) equity option quotes. The implied volatilities of equity options with five year maturity and with moneyness equal to 100% (i.e. at-the-money) are analyzed here.

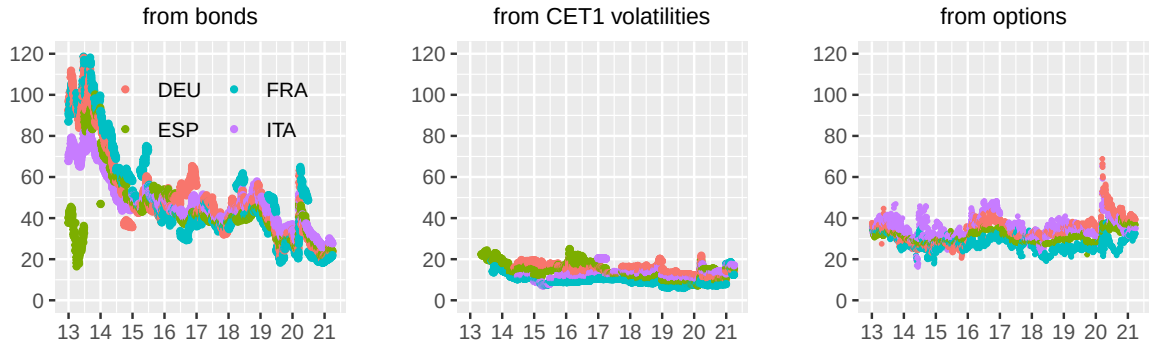

Figure 6: Equity implied volatilities from December 2012 to March 2021 for a subsample of the selected European banks. We report three different implied equity volatilities coming from: (1) the structural model; (2) CET1 ratio volatility and (3) equity option quotes. We consider only banks with the parent company domiciled in Germany (DEU), Spain (ESP), France (FRA) and Italy (ITA). We report the weighted average of the volatilities and the weights are the bank total assets.

By looking at Figure 6, it is clear that the two estimates of the equity implied volatility differ and both volatilities deviate from the equity option implied volatility observed in the market. While these differences are large in the period from the end of 2012 and the end of 2014, starting from 2015 they become less remarkable. In Figure 7, the rolling windows median correlations estimates among the three series of equity volatilities are depicted. Specifically, for each bank, we estimated the correlations using rolling windows of one year length and we computed the median values across all banks. We observe that the median correlation computed across all banks in the sample varies over time. While the correlation is stronger between the equity volatility extracted from CET1 ratios and the other two equity volatilities, the volatility extracted from bonds and that one coming from option data exhibit a low correlation. Assuming that our models are correctly

specified, these empirical findings seem to suggest that there is not a fully coherence among the prices of the different financial products observed in the market or that the information coming from different types of products is not always aligned. Thus, our analysis shows that implied equity volatility estimates depend both on the model and on the financial instruments considered in the calibration.

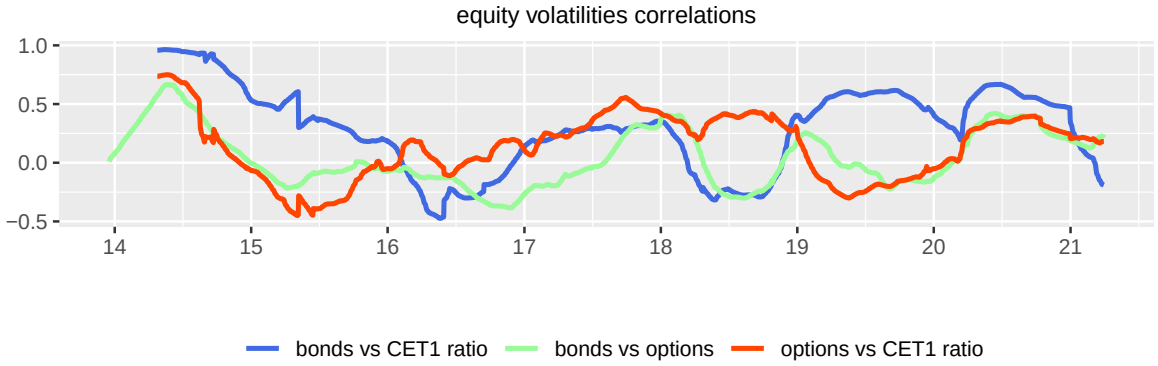

Figure 7: Rolling window correlation between the implied equity volatilities estimated from December 2012 to March 2021 for a subsample of the selected European banks. We consider only banks with the parent company domiciled in Germany (DEU), Spain (ESP), France (FRA) and Italy (ITA). The length of the rolling window is equal to one year. We report the weighted average of the correlation parameters and the weights are the bank total assets.

The differences with respect implied equity volatility derived from option quotes may be due to market misalignments, that is from one side we are considering bond prices from the other side we are looking at equity options. The risk factors influencing the dynamics of these financial instruments are not necessarily the same. Then, as already observed in Section 4, while in the Black and Scholes model the driving process is a geometric Brownian motion, in our structural bond pricing framework the equity is defined as an option. The assumption that the dynamics of the option is a geometric Brownian motion, or simply that equity volatility can be expressed as $\sigma_E E_t$, is an approximation that tries to reconcile the two approaches. Furthermore, in working with structural models, the various liabilities have different maturities, and therefore in bond pricing with structural models a further approximation is introduced. The assumption that CET1 ratio evolves according to a geometric Brownian motion is another approximation that seems reasonable but that cannot be empirically tested. Additionally, the computation of equity implied volatility by means of both the structural and the CET1 ratio models is based on the joint use of market and accounting data. Accounting data are released only on a quarterly basis and this introduces further noises able to partially explain the differences between these implied equity volatilities and the one derived from option prices.

Our empirical results seem to show that the structural model does not fully reconcile with the stochastic CET1 ratio dynamics. Finally, it is to be considered that the liquidity of an equity option decreases as soon as its maturity increases, therefore it can be the case that equity option data refer to broker quotes and not to real market transactions.

Since volatility can be viewed as a measure of risk, our estimates of the asset volatility can be interpreted as an indicator of total assets risk and allow us to investigate banking

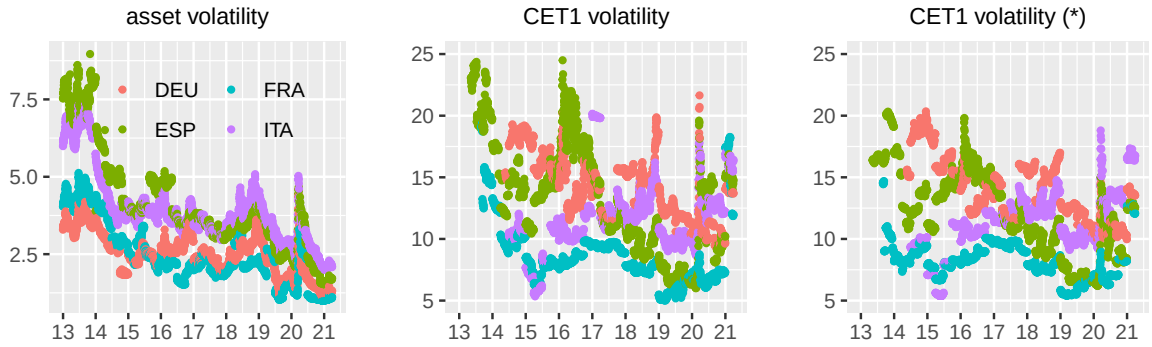

Figure 8: Asset and CET1 ratio implied volatilities from December 2012 to March 2021 for a subsample of the selected European banks. For comparison reasons, the CET1 ratio implied volatilities as defined in De Spiegeleer et al. [2017] are also reported. These volatilities are marked with (*). We consider only banks with the parent company domiciled in Germany (DEU), Spain (ESP), France (FRA) and Italy (ITA). We report the weighted average of the volatilities and the weights are the bank total assets.

fragility at a stand-alone or at a country level. This indicator represents by construction the view of the market on the total assets of a bank and it is based on both market and balance sheet information. As observed by Delis et al. [2021], asset volatility is a key market-based measure of bank portfolio risk and it reflects asset value changes, liability value changes, and other developments in off-balance items and operating efficiency. Our estimates have a magnitude similar to those of Russo et al. [2020b]. It is interesting to observe that, even if the assets of Italian and Spanish banks are perceived as riskier, the differences with respect to the other countries do not seem remarkable, particularly in some periods (see Figure 8)[7]. Asset volatilities change over time and it seems that they reached their highest level before 2014.

Another useful indicator is the CET1 ratio volatility, extracted here on the basis of the bond spreads and of both balance sheet and prudential information. It should be noted that this is an implied volatility and it can be much larger than the historical one.[8] We highlight that implied CET1 ratio volatility varies over time as well and, even with some exceptions, it seems higher for German banks and lower for French ones. For comparison purposes in Figure 8 we report the implied CET1 ratio volatility extracted directly from CoCo bond spreads by following the approach proposed by De Spiegeleer et al. [2017]. There are not large differences between the two estimated implied volatilities. There is not a perfect overlap also because the calibration errors of the two CET1 ratio models are not always zero.

Still in this case the volatility is a measure of risk. The indicator represents the market view on a given bank and this view may not coincide with the risk of the intermediary as measured by the bank risk management or as assessed by supervisors. If two banks have the same CET1 ratio, the higher the CET1 ratio volatility, the riskier the bank. By following a different framework, Russo et al. [2020b] reached the same conclusions.

[7] Note that we are analyzing the major European banks.

[8] According to BBVA [2020] estimates the historical CET1 ratio volatility was below 3% in the period from 2008 to 2020 for a sample of main European banks.

They showed that banks with the same CET1 ratio may have a different probability of breaching capital requirements and, consequently, a different ability to be resilient in order to preserve the capital buffer under stressed conditions. Likewise, banks with a different CET1 ratio may have a similar probability of breaching capital requirements and, consequently, a similar ability to be resilient when facing adverse scenarios. As observed by De Spiegeleer et al. [2017], although a bank improves its CET1 ratio, the market does not necessarily perceive the bank as safer since it is possible that to an increasing CET1 ratio corresponds and increasing CET1 ratio volatility.

7 Risk-neutral and real-world probabilities

In this Section we show how the structural model defined in Section 2 can be used to monitor the dynamics of bank financial soundness. The model allows one to assess the risk of each bank, as perceived by the market, and to investigate banking fragility at a stand-alone or at a country level. By using equations (2.12) and (2.14), it is possible to compute the default probability and the Coco trigger probability, respectively. By construction, the default probability is always lower than the CoCo trigger probability.

Implied risk-neutral and real-world probabilities, if considered in conjunction with a proper dependence structure, can be used as input for the development of a systemic risk indicator (see Kleinow and Moreira [2016], Xu et al. [2017] and Kazato and Yamada [2018]).

7.1 Risk-neutral probabilities

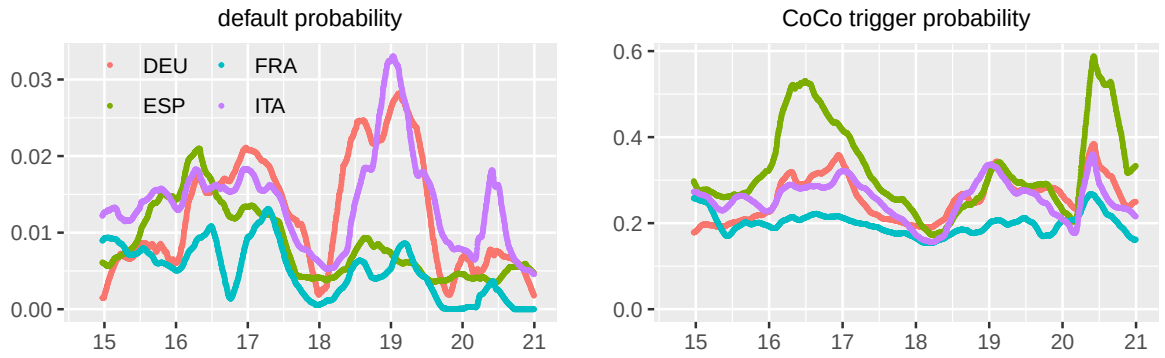

Figure 9: Five-year implied risk-neutral default and CoCo trigger probabilities estimated from December 2014 to December 2020 for a subsample of the selected European banks. We consider only banks with the parent company domiciled in Germany (DEU), Spain (ESP), France (FRA) and Italy (ITA). For each country, first, we compute the weighted average across all banks in the given country, where the weights are the bank total assets. Then, we consider the rolling average evaluated on the basis of the weighted averages of each country. The length of the rolling window is equal to three months.

From a practical standpoint, after defining the model, one has to rely on the calibration described in Section 6.1, which provides the estimated parameters needed to compute the probabilities in equations (2.12) and (2.14).

As in Section 6.2, in Figure 9 we report implied risk-neutral default and CoCo trigger probabilities for four selected countries (Germany, Spain, France, Italy) in the time span from December 2014 to December 2020. For each country, first, we compute the weighted risk-neutral probabilities, obtained by using the bank's total assets as weights of each bank's default and Coco trigger probability. Then, we compute their 3-month rolling averages.

For the reasons discussed in Section 6.1, the quality of the market data before 2014 is not always satisfactory, especially those relating to Cocos of some banks and, therefore, it may affect particularly the estimation of Coco trigger probabilities. For this reason we focus our discussion to the period from December 2014 to December 2020. As far as the risk-neutral default probability is concerned, it is interesting to note that, after 2015 the differences across countries are not remarkable, with the exception between 2018 and 2019, when the probabilities of Italian and German banks were higher in comparison with the other two countries (see Figure 8). These default probabilities change over time.

The dynamics of the CoCo trigger probability is different from the default one. We observe a peak in 2016, during the two stress periods caused by the concerns related to the ability of Deutsche Bank to pay the coupons on its CoCos or even to a possible write-down of their notional value (see Bologna et al. [2020]), and a less pronounced peak between 2018 and 2019 before the overall financial turmoil in March 2020. It appears that for some banks, the shock registered in 2016 was comparable to the shock caused by the Covid-19 outbreak. This empirical finding is also confirmed by the dynamics of the yield of the Bloomberg Barclays Global Coco Banking Euro index around the three peak episodes. The last two peaks are not CoCo specific events but they are due to a negative bank performance observed even on the values of equities, CDS and bonds. At least for the data considered in this study, while the French banks seem to be less risky than their competitors, the Spanish ones seem the most affected during turmoil. This is also caused by the fact that while drops in CoCo prices were similar during turmoil, the residual maturity (or the time until the next call), based on which the yield is evaluated, of the bonds of Spanish banks were much shorter. By looking only at CoCo bonds, the Italian banks are not riskier than the German ones. As expected, the probability of occurrence of a trigger event of CoCo bonds is much higher than the probability of default. It should be observed that for some banks the calibration performance is poor in 2021 (see Figure 4) and this may affect the most recent dynamics of the CoCo trigger probability.

As far as the level of the CoCo trigger probability is concerned, this seems in line with the implied probability estimated by Kazato and Yamada [2018]. By using CoCos prices, they estimated the implied risk-neutral probability reflecting investors belief about the likelihood that a bail-in even would have occurred in the future, and they referred to it as the *bail-in probability*. This probability is similar to the CoCo trigger probability, but its computation is based on the credit derivatives approach originally proposed by De Spiegeleer and Schoutens [2012] which falls in the category of credit risk *reduced form* models. Similarly to Kazato and Yamada [2018], we find that the CoCo risk-neutral trigger probability increases by more than the default probability when events that may lead to a deterioration in the soundness of banks occur. This result suggests that the CoCo trigger probability could be a useful indicator for financial stability monitoring.

7.2 Real-world probabilities

Even if equations (2.12) and (2.14) allow one to estimate the risk-neutral probabilities implied in market quotes, they can be simply adapted to get real-world (or actual) default and Coco trigger probabilities because asset log-return follows a normal distribution with different expectation and the same variance under both probability measures. In particular, by denoting as μ_A the relative drift of the real-world asset process, under the actual probability measure the asset log-return distribution is given by

$$\ln\left(\frac{A_T}{A_t}\right) \sim N\left[(\mu_A - \frac{1}{2}\sigma_A^2)(T-t), \sigma_A^2(T-t)\right],$$

while the risk-neutral one is

$$\ln\left(\frac{A_T}{A_t}\right) \sim N\left[(r - \frac{1}{2}\sigma_A^2)(T-t), \sigma_A^2(T-t)\right].$$

Therefore, to get the actual default probability and the Coco trigger probability formulas it is enough to replace the risk-neutral asset expected log-return on an annual basis, i. e. $r - \frac{1}{2}\sigma_A^2$, in equations (2.12) and (2.14) with the real-world one, i. e. $r_A = \mu_A - \frac{1}{2}\sigma_A^2$. The expected asset log-return can be estimated as the following weighted average

$$r_A = r_E\frac{E}{A} + r_D\frac{D}{A} + r_{ndl}\frac{N_{ndl}}{A}, \tag{7.1}$$

where r_E, r_D, r_{ndl} are the expected return of equity, debt, and non-debt liabilities, while A, E, D, N_{ndl} and are the value of asset, equity, debt, and non-debt libilities, respectively.

It should be noted that all parameters (e.g. σ_A, r_E, and r_D) are estimated at each time t. Aa a possible value of r_E we make use of the return-on-equity (ROE) forecast provided by Institutional Brokers' Estimate System (I/B/E/S). Since the 5-year forward forecasts are not available for all banks in our sample, we consider the 1-year forward forecasts. This data are downloaded from Refinitiv. An estimate of r_D can be obtained by considering the weighted average of senior, subordinated and CoCo bonds yields, with weights given by N_{sen}, N_{sub} and N_{coco}. Furthermore, we assume that expected return on deposit is 0. This is not a restrictive assumption in the analyzed time period. Finally, to implement formula (7.1), the weights are computed by using balance sheet data.

Even if real-world probabilities are lower than risk-neutral one, on average, the level of real-world default and CoCo trigger probabilities is meaningful for all banks in the sample. The median ratio between risk-neutral and actual default (CoCo trigger) probabilities across all banks and over the selected observation window is around 3.2 (1.7).

8 Conclusions

The objective of this paper is fourfold. First, we provide an unified framework in which it is possible to jointly analyze credit spreads, bank balance sheet data and prudential information on capital ratios with the aim to extract three useful indicators of bank risks, that is: asset, equity and CET1 ratio volatilities. Since we model the temporal evolution of bank's asset as a geometric Brownian motion, liabilities and equity prices can be computed using closed formulas, which are obtained by pricing portfolios containing barrier

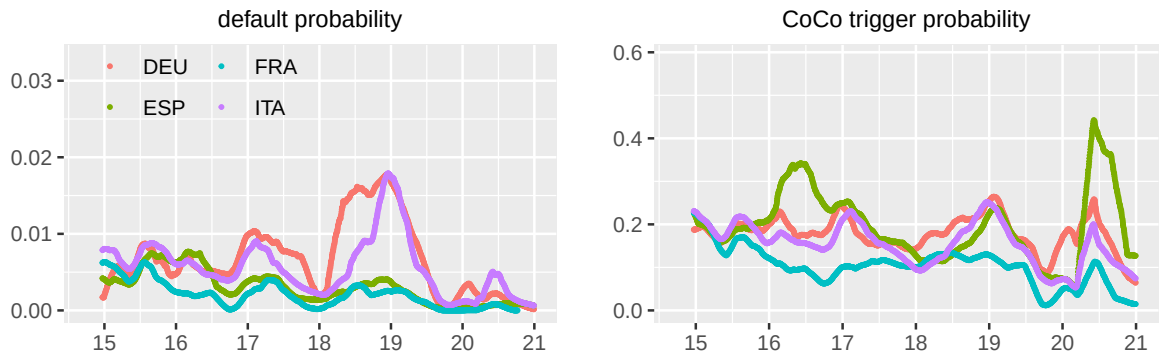

Figure 10: Five-year real-world default and CoCo trigger probabilities estimated from December 2014 to December 2020 for a subsample of the selected European banks. We consider only banks with the parent company domiciled in Germany (DEU), Spain (ESP), France (FRA) and Italy (ITA). For each country, first, we compute the weighted average across all banks in the given country, where the weights are the bank total assets. Then, we consider the rolling average evaluated on the basis of the weighted averages of each country. The length of the rolling window is equal to three months.

options capable of replicating the cash flows produced by the various types of bonds and by the share capital. Second, we show how to connect a possible structural model to the concept of CET1 ratio implied volatility. This connection is obtained through the equality of two different first-passage time probabilities of stochastic processes: the first coming from a structural model, the second from the direct modeling of the CET1 ratio dynamics. Third, we show how to calibrate these models and we conduct an extensive empirical analysis on a sample of the main European banks issuing senior, subordinated and CoCo bonds in the period from December 31, 2012 to March 31, 2021. Even if balance sheet data and the quality of observed spreads may affect the stability of the estimated parameters over time, the proposed model seems to be able to replicate, on average, the credit spreads observed in the market. It should be noted that during stress periods the model reaches the largest calibration errors. Finally, by leveraging on the structural model, it is possible to estimate both the default and the CoCo trigger probability, that is, two indicators useful to explore the dynamics of banking fragility at a stand-alone or at a country level.

The approach described in this contribution could be improved, on the one hand, by describing the evolution of the asset through an exponential Lévy process with jumps and, on the other hand, by considering a stochastic instantaneous risk-free rate. From a theoretical point of view, these extensions should bring a more realistic description of spreads, default and CoCo trigger probabilities. However, empirical analyses of such extended models on real data, and not through sensitivity analysis, are challenging. The limited observability of the total asset value, makes the direct estimation of its dynamics difficult. If one considers a more flexible model and increases the number of parameters, closed formulas are not available, simulation procedures are needed to calibrate the model parameters, and the estimates become less robust. Additionally, the discretization of the time dimension in the simulation of continuous-time processes introduces additional bias. For these reasons, the approach described in this paper seems a good compromise between

tractability and realism.

References

P. Augustin, M.G. Subrahmanyam, D.Y. Tang, and S.Q. Wang. Credit default swaps: Past, present, and future. *Annual Review of Financial Economics*, 8:175–196, 2016.

BBVA. BBVA: a position of strength to address today's challenges and seize future opportunities. *BofA 25th Annual Financials CEO Conference*, September, 2020.

M. Bevilacqua, F. Cannata, S. Cardarelli, R.A. Cristiano, S. Gallina, and M. Petronzi. The evolution of the Pillar 2 framework for banks: some thoughts after the financial crisis. *Occasional Paper, Bank of Italy*, (494), 2019.

M.L. Bianchi and M. Rocco. Disentangling the information content of government bonds and credit default swaps: An empirical analysis on sovereigns and banks. *Frontiers in Applied Mathematics and Statistics*, 2:22, 2016.

F. Black and J.C. Cox. Valuing corporate securities: Some effects of bond indenture provisions. *The Journal of Finance*, 31(2):351–367, 1976.

M.A. Boermans and S. van Wijnbergen. Contingent convertible bonds: Who invests in European CoCos? *Applied Economics Letters*, 25(4):234–238, 2018.

P. Bologna, A. Miglietta, and A. Segura. Contagion in the CoCos market? A case study of two stress events. *International Journal of Central Banking*, 16(6):137–184, 2020.

D. Brigo, J. Garcia, and N. Pede. CoCo bonds pricing with credit and equity calibrated first-passage firm value models. *International Journal of Theoretical and Applied Finance*, 18(3), 2015.

M.P.H. Buergi. Pricing contingent convertibles: a general framework for application in practice. *Financial Markets and Portfolio Management*, 27(1):31–63, 2013.

H. Byström. Stock prices and stock return volatilities implied by the credit market. *The Journal of Fixed Income*, 25(4):32–54, 2016.

G.H. Choe, H.J. Jang, and Y.H. Na. Pricing contingent convertible bonds: An analytical approach based on two-dimensional stochastic processes. *Statistics & Probability Letters*, 148:43–53, 2019.

A. Conciarelli. A new macroprudential tool to assess sources of financial risks: Implied-systemic cost of risks. *International Journal of Finance & Economics*, 19(1):74–88, 2014.

E. Dautović. Has regulatory capital made banks safer? Skin in the game vs moral hazard. *Working Paper, European Central Bank*, (2449), 2020.

J. De Spiegeleer and W. Schoutens. Pricing contingent convertibles: A derivatives approach. *The Journal of Derivatives*, 20(2):27–36, 2012.

J. De Spiegeleer, W. Schoutens, and C. Van Hulle. *The handbook of hybrid securities: Convertible bonds, coco bonds and bail-in*. Wiley, Chichester, 2014.

J. De Spiegeleer, S. Höcht, I. Marquet, and W. Schoutens. CoCo bonds and implied CET1 volatility. *Quantitative Finance*, 17(6):813–824, 2017.

J. De Spiegeleer, I. Marquet, and W. Schoutens. *The risk management of contingent convertible (CoCo) bonds*. Springer, Cham, 2018.

M.D. Delis, S.J. Kim, P.N. Politsidis, and E. Wu. Regulators vs. markets: Are lending terms influenced by different perceptions of bank risk? *Journal of Banking & Finance*, 122:105990, 2021.

M. Derksen, P. Spreij, and S. van Wijnbergen. Accounting noise and the pricing of CoCos. *Discussion Paper*, (12869), 2018.

European Banking Authority. Final report on the implementation of Capital Plans following the EBA's 2011 Recommendation on the creation of temporary capital buffers to restore market confidence, 2012.

S. Forte. Calibrating structural models: a new methodology based on stock and credit default swap data. *Quantitative Finance*, 11(12):1745–1759, 2011.

S. Forte and L. Lovreta. Credit default swaps, the leverage effect, and cross-sectional predictability of equity and firm asset volatility. *Journal of Corporate Finance*, 79: 102347, 2023.

I. Fuentes and J.C. Casado. Contingent convertible bonds and subordinated debt of euro area credit institutions. *Economic Bulletin, Banco de España*, 4, 2017.

P. Glasserman and E. Perotti. The Unconvertible CoCo Bonds. In D.D. Evanoff, G.G. Kaufman, A. Leonello, and S. Manganelli, editors, *Achieving financial stability: Challenges to prudential regulation*, volume 61 of *World Scientific Studies in International Economics*, chapter 23, pages 317–329. World Scientific, Singapore, 2018.

O.J. Grinderslev and K.L. Kristiansen. The information content in contingent convertible bond prices. *Working Paper, Danmarks Nationalbanks*, 122, 2017.

P. Hieber and M. Scherer. A note on first-passage times of continuously time-changed Brownian motion. *Statistics & Probability Letters*, 82(1):165–172, 2012.

J. Hilscher and A. Raviv. Bank stability and market discipline: The effect of contingent capital on risk taking and default probability. *Journal of Corporate Finance*, 29:542–560, 2014.

M. Kazato and T. Yamada. The implied bail-in probability in the contingent convertible securities market. *Monetary and Economic Studies*, 36:57–80, 2018.

B.T. Kelly, G. Manzo, and D. Palhares. Credit-implied volatility. *working paper*, 2019.

Y. S. Kim. Tempered stable process, first passage time, and path-dependent option pricing. *Computational Management Science*, 16(1-2):187–215, 2019.

B.N. Kjell and S.C. Nicolas. Contingent convertible bonds (Cocos) issued by European banks. *Staff Memo, Norges Bank*, (19), 2014.

J. Kleinow and F. Moreira. Systemic risk among European banks: A copula approach. *Journal of International Financial Markets, Institutions and Money*, 42:27–42, 2016.

H. E Leland and K.B. Toft. Optimal capital structure, endogenous bankruptcy, and the term structure of credit spreads. *The Journal of Finance*, 51(3):987–1019, 1996.

P. Li, H. Meng, and F. Yu. Chinese write-down bonds and bank capital structure. *Quantitative Finance*, 18(9):1543–1558, 2018.

P. Li, Y. Han, S. Lin, and T. Qiao. Chinese write-down bonds: issuance and bank capital structure. *Quantitative Finance*, 20(12):2055–2065, 2020.

K. Liberadzki and M. Liberadzki. *Hybrid securities: Structuring, pricing and risk assessment*. Palgrave Macmillan, 2016.

K. Liberadzki and M. Liberadzki. *Contingent convertible bonds, corporate hybrid securities and preferred shares: Instruments, regulation, management*. Palgrave Macmillan, 2019.

F.A. Longstaff and E.S. Schwartz. A simple approach to valuing risky fixed and floating rate debt. *The Journal of Finance*, 50(3):789–819, 1995.

L. Lovreta and F. Silaghi. The surface of implied firms asset volatility. *Journal of Banking & Finance*, 112:105253, 2020.

R.C. Merton. On the pricing of corporate debt: The risk structure of interest rates. *The Journal of Finance*, 29(2):449–470, 1974.

S.K. Nawalkha and R. Rebonato. What interest rate models to use? Buy side versus sell side. *Journal of Investment Management*, 9(3), 2011.

R. Neuberg, P. Glasserman, B. Kay, and S. Rajan. The market-implied probability of European government intervention in distressed banks. *Office of Financial Research, Working Paper*, 16, 2016.

P. Oster. Contingent convertible bond literature review: making everything and nothing possible? *Journal of Banking Regulation*, pages 1–39, 2019.

A. Resti. Bank subordinated debt: a source of capital for lenders or a source of concern for retail investors? *Banca Impresa Società*, 35(1):21–38, 2016.

V. Russo, R. Giacometti, and F.J. Fabozzi. Market implied volatilities for defaultable bonds. *Annals of Operations Research*, 275(2):669–683, 2019.

V. Russo, R. Giacometti, and F.J. Fabozzi. Closed-form solution for defaultable bond options under a two-factor Gaussian model for risky rates modeling. *The Journal of Derivatives*, 28(2):88–103, 2020a.

V. Russo, V. Lagasio, M. Brogi, and F.J. Fabozzi. Application of the Merton model to estimate the probability of breaching the capital requirements under Basel III rules. *Annals of Finance*, 16(1):141–157, 2020b.

O. Vasicek. An equilibrium characterization of the term structure. *Journal of Financial Economics*, 5(2):177–188, 1977.

S. Xu, F. In, C. Forbes, and I. Hwang. Systemic risk in the European sovereign and banking system. *Quantitative Finance*, 17(4):633–656, 2017.

Appendix

A.1 Equity volatility

A.1.1 Model 1

The equity can be priced as a down-and-out call option with threshold level $\alpha_{ndl}N_{ndl}$ and strike L

$$E_t = CB_t^{dout}(\alpha_{ndl}N_{ndl}, L).$$

Since the barrier is strictly smaller than the value of the strike, that is $\alpha_{ndl}N_{ndl} < L$, the equity price is

$$\begin{aligned} E_t &= A_t N(d_1) - Le^{-r(T-t)}N(d_2) \\ &\quad - A_t \left(\frac{\alpha_{ndl}N_{ndl}}{A_t}\right)^{\left(\frac{2r}{\sigma_A^2}+1\right)} N(d_7) + Le^{-r(T-t)}\left(\frac{\alpha_{ndl}N_{ndl}}{A_t}\right)^{\left(\frac{2r}{\sigma_A^2}-1\right)} N(d_8) \\ &= C_t - \left(\frac{\alpha_{ndl}N_{ndl}}{A_t}\right)^{\frac{2r}{\sigma_A^2}} \left[\alpha_{ndl}N_{ndl}N(d_7) - Le^{-r(T-t)}\frac{A_t}{\alpha_{ndl}N_{ndl}}N(d_8)\right] \\ &= C_t - \left(\frac{\alpha L}{A_t}\right)^{\frac{2r}{\sigma_A^2}} \left[\alpha L N(d_7) - e^{-r(T-t)}\frac{A_t}{\alpha}N(d_8)\right], \end{aligned} \tag{A.1}$$

where

$$\begin{aligned} C_t &= A_t N(d_1) - Le^{-r(T-t)}N(d_2), \\ \alpha &= \frac{\alpha_{ndl}N_{ndl}}{L}, \\ d_1 &= \frac{\ln\left(\frac{A_t}{L}\right) + \left(r + \frac{1}{2}\sigma_A^2\right)(T-t)}{\sigma_A\sqrt{T-t}}, \\ d_2 &= \frac{\ln\left(\frac{A_t}{L}\right) + \left(r - \frac{1}{2}\sigma_A^2\right)(T-t)}{\sigma_A\sqrt{T-t}}, \\ d_7 &= \frac{\ln\left(\frac{\alpha^2 L}{A_t}\right) + \left(r + \frac{1}{2}\sigma_A^2\right)(T-t)}{\sigma_A\sqrt{T-t}}, \\ d_8 &= \frac{\ln\left(\frac{\alpha^2 L}{A_t}\right) + \left(r - \frac{1}{2}\sigma_A^2\right)(T-t)}{\sigma_A\sqrt{T-t}}. \end{aligned}$$

Assuming that equity volatility can be expressed as $\sigma_E E_t$ and taking into account that $E_t = f(A_t, \sigma_A)$, an application of Ito's lemma allows to express the relative equity volatility as follows

$$\sigma_E = \frac{dE_t}{dA_t}\frac{A_t}{E_t}\sigma_A,$$

where

$$\frac{dE_t}{dA_t} = N(d_1) - \left(\frac{\alpha L}{A_t}\right)^{\frac{2r}{\sigma_A^2}} \left[\frac{e^{-r(T-t)}}{\alpha}N(d_8)\left(\frac{2r}{\sigma_A^2} - 1\right) - \frac{2r}{\sigma_A^2}\frac{\alpha L N(d_7)}{A_t}\right]. \tag{A.2}$$

Since

$$\frac{dE_t}{dA_t} = \frac{dC_t}{dA_t} - \frac{d}{dA_t}\left(\frac{\alpha L}{A_t}\right)^{\frac{2r}{\sigma_A^2}}\left[\alpha L N(d_7) - e^{-r(T-t)}\frac{A_t}{\alpha}N(d_8)\right],$$

with

$$\frac{dC_t}{dA_t} = N(d_1),$$

$$\begin{aligned}
&\frac{d}{dA_t}\left(\frac{\alpha L}{A_t}\right)^{\frac{2r}{\sigma_A^2}}\left[\alpha L N(d_7) - e^{-r(T-t)}\frac{A_t}{\alpha}N(d_8)\right] \\
&= \left(\frac{\alpha L}{A_t}\right)^{\frac{2r}{\sigma_A^2}}\left[\frac{e^{-r(T-t)}}{\alpha}N(d_8)\left(\frac{2r}{\sigma_A^2} - 1\right) - \frac{2r}{\sigma_A^2}\frac{\alpha L N(d_7)}{A_t}\right] \\
&\quad + \left(\frac{\alpha L}{A_t}\right)^{\frac{2r}{\sigma_A^2}}\left[-\frac{\alpha L N'(d_7)}{A_t\sigma_A\sqrt{T-t}} + \frac{e^{-r(T-t)}}{\alpha}\frac{N'(d_8)}{\sigma_A\sqrt{T-t}}\right].
\end{aligned}$$

Observing that $d_8 = d_7 - \sigma_A\sqrt{T-t}$, we can write

$$N'(d_7 - \sigma_A\sqrt{T-t}) = N'(d_7)\frac{\alpha^2 L}{A_t}\exp\left(r(T-t)\right).$$

Thus, by inserting this expression into $N'(d_8)$, the last term vanishes and we get equation (A.2).

A.1.2 Model 2

The equity price can be expressed as a portfolio of different barrier options. In particular, by defining

$$\begin{aligned}
\Psi_t &= CB_{t,T}^{dout}(K_{coco}, N_{ndl} + N_{sen} + N_{sub} + N_{coco}), \\
\Upsilon_t &= CB_{t,T}^{din}(K_{coco}, N_{ndl} + N_{sen} + N_{sub}), \\
\Phi_t &= CB_{t,T}^{din}(\alpha_{ndl}N_{ndl}, N_{ndl} + N_{sen} + N_{sub}),
\end{aligned}$$

the equity price can be written as

$$E_t = \Psi_t + (1-\gamma)(\Upsilon_t - \Phi_t).$$

Now, we provide the expression of the price of each of the three barrier options and compute their derivative with respect to the asset value. We start with Ψ_t.
Case a) If $K_{coco} > N_{ndl} + N_{sen} + N_{sub} + N_{coco} = L$ (i.e. $\omega > 0$), then

$$\Psi_t = F_t - G_t,$$

where

$$F_t = A_t N(h_3) - Le^{-r(T-t)}N(h_4),$$

$$G_t = \left(\frac{(1+\omega)L}{A_t}\right)^{\frac{2r}{\sigma_A^2}}\left[(1+\omega)LN(h_5) - e^{-r(T-t)}\frac{A_t}{1+\omega}N(h_6)\right],$$

$$K_{coco} = (1+\omega)L,$$

$$h_3 = \frac{\ln\left(\frac{A_t}{(1+\omega)L}\right) + \left(r + \frac{1}{2}\sigma_A^2\right)(T-t)}{\sigma_A\sqrt{T-t}},$$

$$h_4 = \frac{\ln\left(\frac{A_t}{(1+\omega)L}\right) + \left(r - \frac{1}{2}\sigma_A^2\right)(T-t)}{\sigma_A\sqrt{T-t}},$$

$$h_5 = \frac{\ln\left(\frac{(1+\omega)L}{A_t}\right) + \left(r + \frac{1}{2}\sigma_A^2\right)(T-t)}{\sigma_A\sqrt{T-t}},$$

$$h_6 = \frac{\ln\left(\frac{(1+\omega)L}{A_t}\right) + \left(r - \frac{1}{2}\sigma_A^2\right)(T-t)}{\sigma_A\sqrt{T-t}},$$

with

$$\frac{dF_t}{dA_t} = N(h_3) + \frac{N'(h_3)}{\sigma_A\sqrt{T-t}}\left(1 - \frac{1}{1+\omega}\right),$$

$$\frac{dG_t}{dA_t} = \left(\frac{(1+\omega)L}{A_t}\right)^{\frac{2r}{\sigma_A^2}}\left[\frac{e^{-r(T-t)}}{1+\omega}N(h_6)\left(\frac{2r}{\sigma_A^2} - 1\right) - \frac{2r}{\sigma_A^2}\frac{(1+\omega)LN(h_5)}{A_t}\right]$$
$$+ \left(\frac{(1+\omega)L}{A_t}\right)^{\frac{2r}{\sigma_A^2}}\left[\frac{N'(h_5)(1+\omega)L}{A_t\sigma_A\sqrt{T-t}}\left(\frac{1}{1+\omega} - 1\right)\right].$$

and

$$\frac{d\Psi_t}{dA_t} = \frac{dF_t}{dA_t} - \frac{dG_t}{dA_t}.$$

Case b) If $K_{coco} < N_{ndl} + N_{sen} + N_{sub} + N_{coco} = L$ (i.e. $\omega < 0$), then

$$\Psi_t = I_t - H_t,$$

where

$$I_t = A_t N(h_1) - Le^{-r(T-t)}N(h_2),$$

$$H_t = \left(\frac{(1+\omega)L}{A_t}\right)^{\frac{2r}{\sigma_A^2}}\left[(1+\omega)LN(h_7) - e^{-r(T-t)}\frac{A_t}{1+\omega}N(h_8)\right],$$

$$K_{coco} = (1+\omega)L,$$

$$h_1 = \frac{\ln\left(\frac{A_t}{L}\right) + \left(r + \frac{1}{2}\sigma_A^2\right)(T-t)}{\sigma_A\sqrt{T-t}},$$

$$h_2 = \frac{\ln\left(\frac{A_t}{L}\right) + \left(r - \frac{1}{2}\sigma_A^2\right)(T-t)}{\sigma_A\sqrt{T-t}},$$

$$h_7 = \frac{\ln\left(\frac{(1+\omega)^2L}{A_t}\right) + \left(r + \frac{1}{2}\sigma_A^2\right)(T-t)}{\sigma_A\sqrt{T-t}},$$

$$h_8 = \frac{\ln\left(\frac{(1+\omega)^2 L}{A_t}\right) + \left(r - \frac{1}{2}\sigma_A^2\right)(T-t)}{\sigma_A\sqrt{T-t}},$$

with

$$\frac{dI_t}{dA_t} = N(h_1),$$

$$\frac{dH_t}{dA_t} = \left(\frac{(1+\omega)L}{A_t}\right)^{\frac{2r}{\sigma_A^2}} \left[\frac{e^{-r(T-t)}}{1+\omega} N(h_8)\left(\frac{2r}{\sigma_A^2} - 1\right) - \frac{2r}{\sigma_A^2}\frac{(1+\omega)LN(h_7)}{A_t}\right].$$

To resume

$$\frac{d\Psi_t}{dA_t} = \frac{dI_t}{dA_t} - \frac{dH_t}{dA_t}.$$

Now we consider Υ_t.

Case c) If $K_{coco} = (1+\omega)L > N_{ndl} + N_{sen} + N_{sub} = L - N_{coco}$, then

$$\Upsilon_t = O_t + P_t + Q_t$$

where

$$O_t = A_t N(t_1) - (L - N_{coco})e^{-r(T-t)}N(t_2),$$

$$P_t = \left(\frac{(1+\omega)L}{A_t}\right)^{\frac{2r}{\sigma_A^2}} \left[(1+\omega)LN(t_5) - (L - N_{coco})e^{-r(T-t)}\frac{A_t}{(1+\omega)L}N(t_6)\right],$$

$$Q_t = (L - N_{coco})e^{-r(T-t)}N(t_4) - A_t N(t_3),$$

$$t_1 = \frac{\ln\left(\frac{A_t}{L-N_{coco}}\right) + \left(r + \frac{1}{2}\sigma_A^2\right)(T-t)}{\sigma_A\sqrt{T-t}},$$

$$t_2 = \frac{\ln\left(\frac{A_t}{L-N_{coco}}\right) + \left(r - \frac{1}{2}\sigma_A^2\right)(T-t)}{\sigma_A\sqrt{T-t}},$$

$$t_3 = \frac{\ln\left(\frac{A_t}{(1+\omega)L}\right) + \left(r + \frac{1}{2}\sigma_A^2\right)(T-t)}{\sigma_A\sqrt{T-t}},$$

$$t_4 = \frac{\ln\left(\frac{A_t}{(1+\omega)L}\right) + \left(r - \frac{1}{2}\sigma_A^2\right)(T-t)}{\sigma_A\sqrt{T-t}},$$

$$t_5 = \frac{\ln\left(\frac{(1+\omega)L}{A_t}\right) + \left(r + \frac{1}{2}\sigma_A^2\right)(T-t)}{\sigma_A\sqrt{T-t}},$$

$$t_6 = \frac{\ln\left(\frac{(1+\omega)L}{A_t}\right) + \left(r - \frac{1}{2}\sigma_A^2\right)(T-t)}{\sigma_A\sqrt{T-t}}.$$

Thus,

$$\frac{dO_t}{dA_t} = N(t_1),$$

$$\frac{dQ_t}{dA_t} = -N(t_3) - \frac{N'(t_3)}{\sigma_A\sqrt{T-t}}\left(1 - \frac{L - N_{coco}}{(1+\omega)L}\right),$$

$$\frac{dP_t}{dA_t} = \left(\frac{(1+\omega)L}{A_t}\right)^{\frac{2r}{\sigma_A^2}}\left[\frac{(L-N_{coco})e^{-r(T-t)}}{(1+\omega)L}N(t_6)\left(\frac{2r}{\sigma_A^2} - 1\right) - \frac{2r}{\sigma_A^2}\frac{(1+\omega)LN(t_5)}{A_t}\right]$$
$$+ \left(\frac{(1+\omega)L}{A_t}\right)^{\frac{2r}{\sigma_A^2}}\left[\frac{N'(t_5)(1+\omega)L}{A_t\sigma_A\sqrt{T-t}}\left(\frac{L - N_{coco}}{(1+\omega)L} - 1\right)\right],$$

and therefore

$$\frac{d\Upsilon_t}{dA_t} = \frac{dO_t}{dA_t} + \frac{dQ_t}{dA_t} + \frac{dP_t}{dA_t}.$$

Case d) If $K_{coco} = (1+\omega)L < N_{ndl} + N_{sen} + N_{sub} = L - N_{coco}$, then

$$\Upsilon_t = R_t,$$

where

$$R_t = \left(\frac{(1+\omega)L}{A_t}\right)^{\frac{2r}{\sigma_A^2}}\left[(1+\omega)LN(t_7) - (L-N_{coco})e^{-r(T-t)}\frac{A_t}{(1+\omega)L}N(t_8)\right],$$

$$t_7 = \frac{\ln\left(\frac{(1+\omega)^2L^2}{A_t(L-N_{coco})}\right) + \left(r + \frac{1}{2}\sigma_A^2\right)(T-t)}{\sigma_A\sqrt{T-t}},$$

$$t_8 = \frac{\ln\left(\frac{(1+\omega)^2L^2}{A_t(L-N_{coco})}\right) + \left(r - \frac{1}{2}\sigma_A^2\right)(T-t)}{\sigma_A\sqrt{T-t}}.$$

Thus,

$$\frac{dR_t}{dA_t} = \left(\frac{(1+\omega)L}{A_t}\right)^{\frac{2r}{\sigma_A^2}}\left[\frac{(L-N_{coco})e^{-r(T-t)}}{(1+\omega)L}N(t_8)\left(\frac{2r}{\sigma_A^2} - 1\right) - \frac{2r}{\sigma_A^2}\frac{(1+\omega)LN(t_7)}{A_t}\right],$$

and therefore

$$\frac{d\Upsilon_t}{dA_t} = \frac{dR_t}{dA_t}.$$

Finally we consider Φ_t. Since we impose

$$\alpha_{ndl}N_{ndl} = \alpha L < N_{ndl} + N_{sen} + N_{sub} = L - N_{coco},$$

we have

$$\Phi_t = \left(\frac{\alpha L}{A_t}\right)^{\frac{2r}{\sigma_A^2}}\left[\alpha LN(s_7) - e^{-r(T-t)}\frac{A_t(L-N_{coco})}{\alpha L}N(s_8)\right],$$

where

$$s_7 = \frac{\ln\left(\frac{\alpha^2L^2}{A_t(L-N_{coco})}\right) + \left(r + \frac{1}{2}\sigma_A^2\right)(T-t)}{\sigma_A\sqrt{T-t}},$$

$$s_8 = \frac{\ln\left(\frac{\alpha^2L^2}{A_t(L-N_{coco})}\right) + \left(r - \frac{1}{2}\sigma_A^2\right)(T-t)}{\sigma_A\sqrt{T-t}}.$$

$$\begin{aligned}\frac{d\Phi_t}{dA_t} &= \left(\frac{\alpha L}{A_t}\right)^{\frac{2r}{\sigma_A^2}} \left[\frac{e^{-r(T-t)}(L-N_{coco})}{\alpha L} N(s_8)\left(\frac{2r}{\sigma_A^2}-1\right) - \frac{\alpha L N(s_7)}{A_t}\right] \\ &+ \left(\frac{\alpha L}{A_t}\right)^{\frac{2r}{\sigma_A^2}} \left[-\frac{\alpha L N'(s_7)}{A_t \sigma_A \sqrt{T-t}} + \frac{e^{-r(T-t)}(L-N_{coco})}{\alpha L}\frac{N'(s_8)}{\sigma_A\sqrt{T-t}}\right] \\ &= \left(\frac{\alpha L}{A_t}\right)^{\frac{2r}{\sigma_A^2}} \left[\frac{e^{-r(T-t)}(L-N_{coco})}{\alpha L} N(s_8)\left(\frac{2r}{\sigma_A^2}-1\right) - \frac{\alpha L N(s_7)}{A_t}\right],\end{aligned}$$

because the last term is equal to zero since

$$N'(s_8 - \sigma_A\sqrt{T-t}) = N'(s_7)\frac{\alpha^2 L^2}{A_t(L-N_{coco})}e^{r(T-t)}.$$

To resume

$$\frac{dE_t}{dA_t} = \frac{d\Psi_t}{dA_t} + (1-\gamma)\left(\frac{d\Upsilon_t}{dA_t} - \frac{d\Phi_t}{dA_t}\right).$$

A.2 CET1 volatility

In this Section we describe how to obtain the CET1 implied volatility starting from the yield of CoCo bonds observed in the market. Here the write down is defined as the first time in which the CET1 process hits the trigger level $Trigger$ observed at time t.

We assume that asset and equity are correlated geometric Brownian motions under the physical probability measure

$$dA_t = \mu_A A_t dt + \sigma_A A_t dW_{1t},$$

and

$$dE_t = \mu_E E_t dt + \sigma_E E_t(\rho dW_{1t} + \sqrt{1-\rho^2}dW_{2t}),$$

where W_{1t} and W_{2t} are standard Brownian motions with correlation $\rho(W_{1t}, W_{2t}) = 0$, and that the risk density is a constant w observed at time t, that is

$$CET1_t = \frac{E_t}{wA_t} = \frac{1}{w}\frac{E_t}{A_t} = \frac{1}{w}EAR_t$$

where EAR_t is the equity-asset ratio at time t.

Applying Itô's lemma, we get the dynamics of the equity-asset ratio

$$\begin{aligned}d\left(\frac{E_t}{A_t}\right) =& (\mu_E - \mu_A + \sigma_A^2 - \rho\sigma_E\sigma_A)\frac{E_t}{A_t}dt + \\ &+ \left((\rho\sigma_E - \sigma_A)dW_{1t} + \sigma_E\sqrt{1-\rho^2}dW_{2t}\right)\frac{E_t}{A_t}.\end{aligned} \tag{A.3}$$

Since

$$(\rho\sigma_E - \sigma_A)dW_{1t} + \sigma_E\sqrt{1-\rho^2}dW_{2t} \sim N\left(0, (\sigma_A^2 + \sigma_E^2 - 2\rho\sigma_A\sigma_E)dt\right),$$

we can set

$$\sqrt{\sigma_A^2 + \sigma_E^2 - 2\rho\sigma_A\sigma_E}dW_{3t} = (\rho\sigma_E - \sigma_A)dW_{1t} + \sigma_E\sqrt{1-\rho^2}dW_{2t},$$

and write $(A.3)$ as a geometric Brownian motion

$$dEAR_t = \mu_{EAR} EAR_t dt + \sigma_{EAR} EAR_t dW_{3t}.$$

where

$$\mu_{EAR} = \mu_E - \mu_A + \sigma_A^2 - \rho\sigma_E\sigma_A,$$

and

$$\sigma_{EAR} = \sqrt{\sigma_A^2 + \sigma_E^2 - 2\rho\sigma_A\sigma_E},$$

Thus, we get

$$\begin{aligned} dCET1_t &= \frac{1}{w}\left(\mu_{EAR} EAR_t dt + \sigma_{EAR} EAR_t dW_{3t}\right), \\ &= \mu_{CET1}\, CET1_t dt + \sigma_{CET1}\, CET1_t dW_{3t}. \end{aligned}$$

where

$$\mu_{CET1} = \mu_{EAR}, \tag{A.4}$$

and

$$\sigma_{CET1} = \sigma_{EAR}, \tag{A.5}$$

So we can write

$$CET1_T = CET1_t \exp\left[\left(\mu_{CET1} - \frac{1}{2}\sigma_{CET1}^2\right)(T-t) + \sigma_{CET1} W_{3(T-t)}\right]$$

and the probability related to the CET1 hitting time is given by

$$\begin{aligned} p(t < \tau_{cet1} < T) &= N\left(\frac{\ln(\frac{Trigger}{CET1_t}) - (\mu_{CET1} - \frac{1}{2}\sigma_{CET1}^2)(T-t)}{\sigma_{CET1}\sqrt{T-t}}\right) \\ + \left(\frac{Trigger}{CET1_t}\right)^{2\frac{\mu_{CET1} - \frac{1}{2}\sigma_{CET1}^2}{\sigma_{CET1}^2}} & N\left(\frac{\ln(\frac{Trigger}{CET1_t}) + (\mu_{CET1} - \frac{1}{2}\sigma_{CET1}^2)(T-t)}{\sigma_{CET1}\sqrt{T-t}}\right) \end{aligned} \tag{A.6}$$

Under the risk neutral measure, since $\mu_A = \mu_E = r$, the CET1 ratio process has drift

$$\mu_{CET1} = \sigma_A^2 - \rho\sigma_E\sigma_A.$$